© 2016. Published by The Company of Biologists Ltd | Development (2016) 143, 3481-3490 doi:10.1242/dev.131466

STEM CELLS AND REGENERATION

RESEARCH ARTICLE

Activation of Smad2 but not Smad3 is required to mediate TGF-β signaling during axolotl limb regeneration

Jean-François Denis[1], Fadi Sader[1], Samuel Gatien[1], Éric Villiard[2], Anie Philip[3] and Stéphane Roy[1,2,*]

ABSTRACT

Axolotls are unique among vertebrates in their ability to regenerate tissues, such as limbs, tail and skin. The axolotl limb is the most studied regenerating structure. The process is well characterized morphologically; however, it is not well understood at the molecular level. We demonstrate that TGF-β1 is highly upregulated during regeneration and that TGF-β signaling is necessary for the regenerative process. We show that the basement membrane is not prematurely formed in animals treated with the TGF-β antagonist SB-431542. More importantly, Smad2 and Smad3 are differentially regulated post-translationally during the preparation phase of limb regeneration. Using specific antagonists for Smad2 and Smad3 we demonstrate that Smad2 is responsible for the action of TGF-β during regeneration, whereas Smad3 is not required. Smad2 target genes (*Mmp2* and *Mmp9*) are inhibited in SB-431542-treated limbs, whereas non-canonical TGF-β targets (e.g. *Mmp13*) are unaffected. This is the first study to show that Smad2 and Smad3 are differentially regulated during regeneration and places Smad2 at the heart of TGF-β signaling supporting the regenerative process.

KEY WORDS: Axolotl, Epimorphic, Regeneration, TGF-β signaling, Smad2, Smad3, Limb, Salamander, Urodeles, *Ambystoma mexicanum*

INTRODUCTION

The capacity to regenerate complex tissues and organs as adults is a process exhibited by few vertebrates. In fact, urodeles (e.g. axolotls and newts) are the only tetrapods that can regenerate multiple tissues throughout their life. The urodele limb represents an ideal structure for understanding the signals modulating the process of epimorphic regeneration in vertebrates. The stages of limb regeneration are well characterized (Iten and Bryant, 1973; Tank et al., 1976) and animals tolerate the surgery extremely well. Limb regeneration represents a highly orchestrated series of cellular and molecular events that control cellular migration and proliferation, as well as the initial wound healing phase. The process is often subdivided into two general phases: (1) a preparation phase immediately following amputation, comprising wound epithelium formation, cellular dedifferentiation, migration and proliferation giving rise to the blastema; and (2) a redevelopment phase, which is generally considered to initiate around the late bud stage of blastema formation and corresponds to when regeneration becomes nerve independent, cellular redifferentiation starts in parallel with pattern formation and cells stop proliferating (Tank et al., 1976; Wallace, 1981; Gardiner et al., 1999).

The preparation phase of limb regeneration shares similarities with mammalian wound healing during the first 48-72 h post-amputation/wounding (Roy and Lévesque, 2006; Denis et al., 2013). Both are characterized by the migration of epidermal cells to cover the wound, the upregulation of extracellular matrix (ECM) remodeling proteins, the appearance of some inflammatory markers and the activation of dermal fibroblasts to migrate under the wound epithelium (Yang and Bryant, 1994; Yang et al., 1999a; Han et al., 2005; Godwin et al., 2013). To understand how axolotls can regenerate lost body parts, it is important to determine which specific molecular pathways of the normal wound healing response observed in non-regenerating models are present in this regenerating organism. It is also important to determine the regulation and function of the different components of such pathways in a situation of complete regeneration.

A previous study demonstrated that the level of *Tgf-β1* mRNA was upregulated early following amputation (already upregulated at 6 h) and that expression remained high until early bud stage, when it returned to normal (Levesque et al., 2007). In that same study, SB-431542, which is a chemical antagonist of TGF-β receptor type I (TβR-I) (Inman et al., 2002), was used to specifically inhibit TGF-β signaling. This demonstrated, for the first time, that TGF-β signaling is necessary for the cellular proliferation that gives rise to the blastema and limb regeneration. TGF-β signaling is important during development, wound healing, bone fracture healing and in compensatory liver hyperplasia following partial hepatectomy (Braun et al., 1988; Zentella and Massague, 1992; Massague, 2000; Gabbiani, 2003). Interestingly, TGF-β1 has also been shown to regulate matrix metalloproteinases (MMPs), tissue inhibitors of MMPs (TIMPs) (Overall et al., 1991; Sehgal and Thompson, 1999; Blavier et al., 2001) and fibronectin in several species, including axolotls (Zhao, 1999; Levesque et al., 2007). The Smad transcription factors represent the major intracellular mediators of TGF-β superfamily signaling. There are eight Smads in mammals (Smad1-8) responsible for transmitting the TGF-β superfamily response from the cell surface receptors to the nucleus (Massague and Chen, 2000; Wrana and Attisano, 2000; Attisano and Wrana, 2002; Derynck and Zhang, 2003). Smads are divided into three types: receptor Smads (R-Smads), which are phosphorylated by TβR-I; co-Smad (Smad4), which heterodimerizes with R-Smads to induce transcription; and inhibitory Smads (I-Smads), which block the phosphorylation of R-Smads. TGF-βs and BMPs utilize different subsets of cell surface receptors as well as different Smads to transmit their signals. The TGF-β isoforms 1-3 signal via R-Smads 2 and 3 and are negatively controlled by I-Smad7. Canonical TGF-β signaling involves the phosphorylation of two serines in the C-terminus of both Smad2 and Smad3 by TβR-I (Zhang et al., 1996; Nakao et al., 1997). BMPs signal via R-Smads 1, 5 and 8 and are

[1]Department of Biochemistry and Molecular Medicine, Faculty of Medicine, Université de Montréal, Montréal, Québec, H3C-3J7, Canada. [2]Department of Stomatology, Faculty of Dentistry, Université de Montréal, Montréal, Québec, H3C-3J7, Canada. [3]Department of Surgery, Faculty of Medicine, McGill University, Montréal, Québec, H3G-1A4, Canada.

*Author for correspondence (stephane.roy@umontreal.ca)

S.R., 0000-0002-4504-0968

Received 2 October 2015; Accepted 8 August 2016

Development (2016) 143, 3481-3490 doi:10.1242/dev.131466

negatively controlled by I-Smad6. Smad4 is the co-Smad for all the R-Smads and is used for TGF-β and BMPs. There are also non-canonical TGF-β signaling pathways that are mediated via the mitogen-activated protein kinases, such as p38 and Jun-k, and phosphatidylinositol-3-kinase/Akt (Zhang, 2009; Mu et al., 2012).

Limb regeneration shares many similarities with limb development, including the interaction of epithelial and mesenchymal cells (Neufeld and Aulthouse, 1986). This interaction requires the absence of a basement membrane between these two cell types, at least during the initial stages of regeneration. During limb regeneration, Neufeld and co-workers showed that the basement membrane was not re-established early during the regenerative process, allowing interactions between epithelial and mesenchymal cells (Neufeld and Day, 1996; Neufeld et al., 1996). The idea that blocking TGF-β signaling leads to the premature establishment of the basal membrane, thereby preventing the wound epithelium from being permissive, is the first thing that we assessed in the present study. Also, in order to determine how TGF-β controls limb regeneration, a better understanding of the intracellular components of the pathway is needed. Various Smad knockout (KO) mice have been generated: *Smad2* and *Smad4* KOs were lethal, whereas the *Smad3* KO was viable (Nomura and Li, 1998; Sirard et al., 1998; Waldrip et al., 1998; Weinstein et al., 1998; Zhu et al., 1998; Datto et al., 1999; Yang et al., 1999b). The phenotype of *Smad3* KO mice was interesting in multiple ways: (1) mice were viable and relatively normal (Datto and Wang, 2000); (2) the TGF-β response was somewhat amplified in fibroblasts, which is contrary to what one would expect for an R-Smad KO (Piek et al., 2001); (3) they displayed improved wound healing capacities for various types of injury, which were marked by an increased rate of re-epithelialization and significantly reduced scarring (Ashcroft et al., 1999; Flanders et al., 2003; Falanga et al., 2004); and (4) they had less inflammation following skin wounding (Ashcroft et al., 1999; Yang et al., 1999b; Ashcroft and Roberts, 2000). All of these changes observed in the *Smad3* KO mice, as compared with their wild-type littermates, actually display a striking resemblance to the early phases of regeneration in axolotls (Roy and Lévesque, 2006). This also highlights the fact that Smad2 and Smad3 play different roles in mediating TGF-β signaling. Smad3 is associated with scarring and the inhibition of proliferation, whereas Smad2 is associated with cellular migration and proliferation (Brown et al., 2007). These functions are not simultaneously compatible with the regenerative process. Scarring is absent during limb regeneration, while proliferation and cellular migration are necessary during the preparation phase (Wallace, 1981; Levesque et al., 2007).

The present study focuses on the role of Smad2 and Smad3, as the mediators of the canonical TGF-β signaling pathway, during the early phase of limb regeneration in axolotl. Newly available reagents made it possible to determine whether Smad2 and Smad3 are activated during limb regeneration and to what extent their individual roles are important in this process.

RESULTS

The basement membrane is not prematurely restored by TGF-β inhibition

It was previously shown that cellular proliferation is blocked by the TGF-β antagonist SB-431542 (Levesque et al., 2007). The same study also showed that 7 days of treatment is enough to prevent regeneration, even when treatment is then stopped. However, wound closure was not noticeably affected. Hence, we wondered whether the basement membrane was restored prematurely in treated animals, thereby inhibiting signaling between the apical epithelial cap (AEC) and the underlying mesenchymal cells. This could explain, in part, the loss in cellular proliferation of mesenchymal cells observed when TGF-β signaling is blocked. In order to assess restoration of the basement membrane, we took advantage of Picrosirius Red staining, which is specific for collagens (Junqueira et al., 1978, 1979; Kiraly et al., 1997).

Collagens in the basement membrane were not detectable at the amputated extremity 6 days post-amputation in control or treated limbs (Fig. 1B,E). To confirm the lack of a basement membrane under the AEC, the expression of Col IV protein, a specific marker of basement membrane (Kuhn, 1995; Poschl et al., 2004), was assessed. As shown in Fig. 1C,C′,F,F′, Col IV is not present under the AEC site 6 days post-amputation in either controls or SB-431542-treated animals. Other time points (as shown in Fig. S1) demonstrated that, even as late as medium bud or palette stage, the basement membrane is not reformed prematurely in SB-431542-treated animals. Therefore, the lack of proliferation observed in SB-431542-treated limbs is not due to the premature formation of basement membrane.

Cloning of *Smad2*, *Smad3* and *Smad7*

Since TGF-β signaling is essential for regeneration and blastema formation, regulation of the intracellular components of the canonical pathway was assessed. Canonical signaling occurs through the C-terminal phosphorylation of serine residues of Smad2 and Smad3. Full-length cDNAs were cloned for *Smad2* and *Smad3* (GenBank accessions KT383019 and KT383020), as well as a partial clone for *Smad7* (see the supplementary Materials and Methods). Of particular interest was the C-terminal portion of Smad2 and Smad3 that contains the SSVS motif, which is phosphorylated twice for activation (Massague et al., 2005). The sequence identity of axolotl proteins compared with human is 99% (464/467 amino acids) for Smad2 and 93% (402/432 amino acids) for Smad3, showing that these proteins are highly conserved (Figs S2 and S3) over a vast phylogenetic distance from urodeles to humans, spanning 370 million years (Smith and Voss, 2006).

Involvement of Smads and TGF-β signaling in normal regeneration

RT-PCR and western blotting (Smad2 and Smad3) analyses were performed to assess the expression of Smads and the phosphorylation of the Smad C-terminal SSVS motif during regeneration. Commercially available antibodies were used for all proteins except for phosphorylated axolotl Smad3 (p-Smad3), which was not recognized by most commercial antibodies. The Biorbyt S425 p-Smad3 antibody (orb222846) did cross react with the axolotl protein but only recognizes one phosphorylation site. An in-house mouse polyclonal antibody was raised against a 12 amino acid phospho-peptide identical in sequence to the last 12 amino acids of the axolotl p-Smad3 protein. No antibodies were found that cross-reacted against the axolotl Smad7 protein.

The results show that *Smad2*, *Smad3* and *Smad7* do not differ significantly at the mRNA level during the preparation phase of limb regeneration (Fig. 2A). Expression of *Smad2*, *Smad3* and *Smad7* mRNA did, however, show an upregulation during the redevelopment phase. The timing of this upregulation correlates with an accumulation of cells in the regenerative process (Wallace, 1981). *Tgf-β2*, *Activin* and *Smad4* mRNA levels were not upregulated (data not shown). Since RT-PCR measures mRNA levels, findings may correlate with total protein levels but are not informative regarding potential post-translational modifications. Indeed, Smad2 and Smad3 are known targets for post-translational

Development (2016) 143, 3481-3490 doi:10.1242/dev.131466

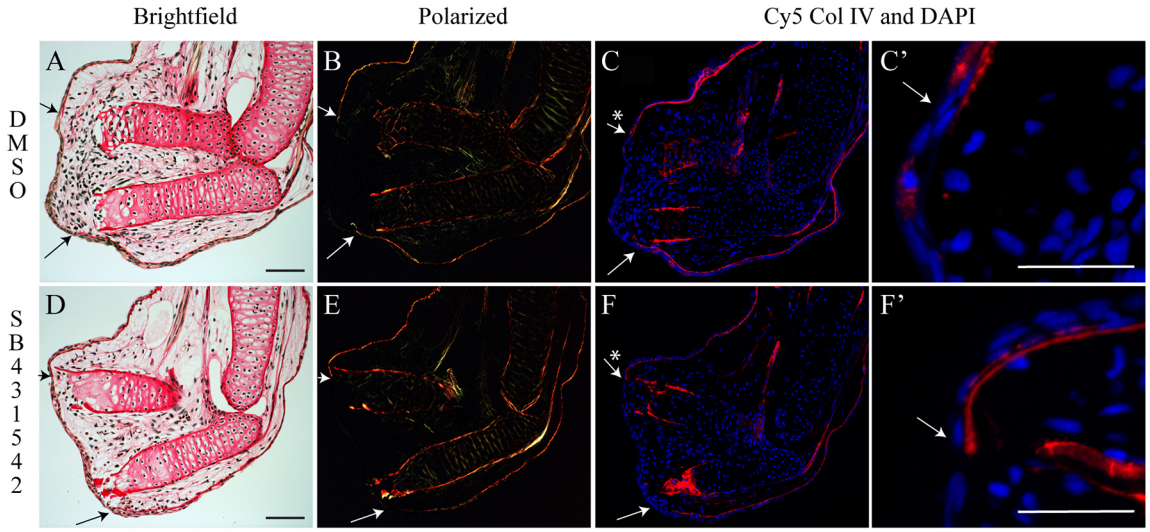

Fig. 1. The basement membrane does not prematurely reform when TGF-β signaling is blocked in regenerating axolotl limbs. (A-C′) Control animal, DMSO treated for 6 days post-amputation. (A,B) Picrosirius Red staining showing normal blastema formation in brightfield view (A) and polarized light (B); collagen fibers light up red/orange/green. The basement membrane is not restored. (C,C′) Col IV (basement membrane protein) expression (red) confirms that the basement membrane is not restored (no Col IV is present in the regenerating portion, asterisk). DAPI (blue), showing cell nuclei. C′ is a magnification from C. (D-F′) Animal treated with 25 µM SB-431542 for 6 days post-amputation. (D,E) Picrosirius Red staining showing no blastema formation (no cells have accumulated under the wound epidermis) in treated limb in brightfield view (D) and polarized light (E). The basement membrane is not restored. (F,F′) Col IV expression confirms that the basement membrane is not restored 6 days post-amputation under SB-431542 treatment (no Col IV is present in the regenerating portion, asterisk). F′ is a magnification from F. Composite images are shown. Arrows indicate the base of the blastema corresponding to the amputation site. *n*=5 for Picrosirius Red staining; *n*=3 for Col IV immunofluorescence. Scale bars: 200 µm in A,D; 90 µm in C′,F′.

modifications (e.g. S-phosphorylation at the C-terminus) and these could play a role in blastema formation. Western blot experiments looking at total and phosphorylated Smad proteins were conducted. Results show maximal expression of active TGF-β1 (12.5 kDa fragment) between 6 h and 48 h (Fig. 2B). Protein expression matches the mRNA expression of *Tgf-β1* described previously (Levesque et al., 2007). Total Smad2 protein levels were reduced during the preparation phase but elevated during redevelopment, which correlates with the RT-PCR results (Fig. 2C). Phosphorylation of Smad2 was detected between 6 h and 48 h, which correspond to the time when mesenchymal cells migrate and begin to proliferate to give rise to the blastema. This also correlates with maximal expression of active TGF-β1 (Fig. 2C). Total Smad3 protein levels were also reduced during the preparation phase but elevated during redevelopment, correlating with the RT-PCR results (Fig. 2D). Phosphorylation of Smad3 was detected from 3 h to 24 h post-amputation (Fig. 2E-G). Phosphorylation of Smad3 occurs before phosphorylation of Smad2, while the wound is closing. Interestingly, detection of p-Smad3 required a very sensitive reagent, SignalFire Elite ECL Reagent (Cell Signaling), which is six to seven times more sensitive than the ECL reagent Lumi-Light^{Plus} (Roche) used to detect p-Smad2 (data not shown). p-Smad3 was undetectable, or very difficult to detect, with the reagent used to detect p-Smad2 (Fig. 2C,E). Consequently, the level of p-Smad3 is likely to be minimal compared with p-Smad2 during regeneration. These differences were unlikely to be due to the antibodies used, as our mouse polyclonal and the Biorbyt commercial antibody yielded identical results. These data suggest a differential activation of Smad proteins during regeneration.

Inhibition of Smad2 but not Smad3 phosphorylation prevents regeneration

Activation of Smad proteins is likely to be essential for regeneration, as treatment with SB-431542 prevents blastema formation and blocks regeneration (Levesque et al., 2007). SB-431542 is an inhibitor of TGF-β signaling that acts at the receptor level, thus preventing phosphorylation of its targets (Smad2 and Smad3). Our results indeed show a strong inhibition (≥85%) of Smad2 phosphorylation at 24 h post-amputation in animals treated with 25 µM SB-431542 (Fig. 3B,D). Phosphorylation of Smad3 at 3 h post-amputation is also inhibited (≥53%) when animals are treated with 25 µM SB-431542 (Fig. 3A,C). Hence, we took advantage of a second inhibitor, SIS3, which is specific to Smad3 phosphorylation. Animals were treated with 4 µM, 3 µM and 2 µM SIS3 for 35 days. Results show that inhibiting Smad3 phosphorylation does not prevent regeneration. All animals treated with 4 µM SIS3 died before the end of treatment; however, they all showed a perfectly normal blastema, as in the size-matched controls (data not shown). Half of the animals treated with 3 µM SIS3 died after 20 days of treatment, but again showed blastemas similar to those of control animals at the time of death. Animals that survived the 35-day treatment regenerated their limbs to near perfection, with only a few carpal elements missing in some of the limbs (three of four limbs analyzed were missing one or two carpal elements) (Fig. 3G,J). No delays in limb regeneration were observed in animals treated with 2 µM SIS3 (100% survival rate; five out of eight limbs analyzed showed one or two missing carpal elements) (Fig. 3F,I). Nevertheless, p-Smad3 was diminished by more than 46% with SIS3 treatment, as assessed by western blot analysis (Fig. 3C). Smad2 phosphorylation was unaffected by SIS3 treatment, whereas it was greatly inhibited following SB-431542 treatment (Fig. 3D). In addition, a third inhibitor of Smad3, Naringenin, was tested to see whether it would have the same effects as SIS3. We selected the highest dose that did not affect the health and growth of animals when treated daily for 35 days (data not shown). When treated with 35 µM Naringenin, animals regenerated perfectly. p-Smad3, measured 6 h post-amputation, was reduced by 51%, whereas p-Smad2 levels were not reduced by Naringenin treatment (data not shown).

Development (2016) 143, 3481-3490 doi:10.1242/dev.131466

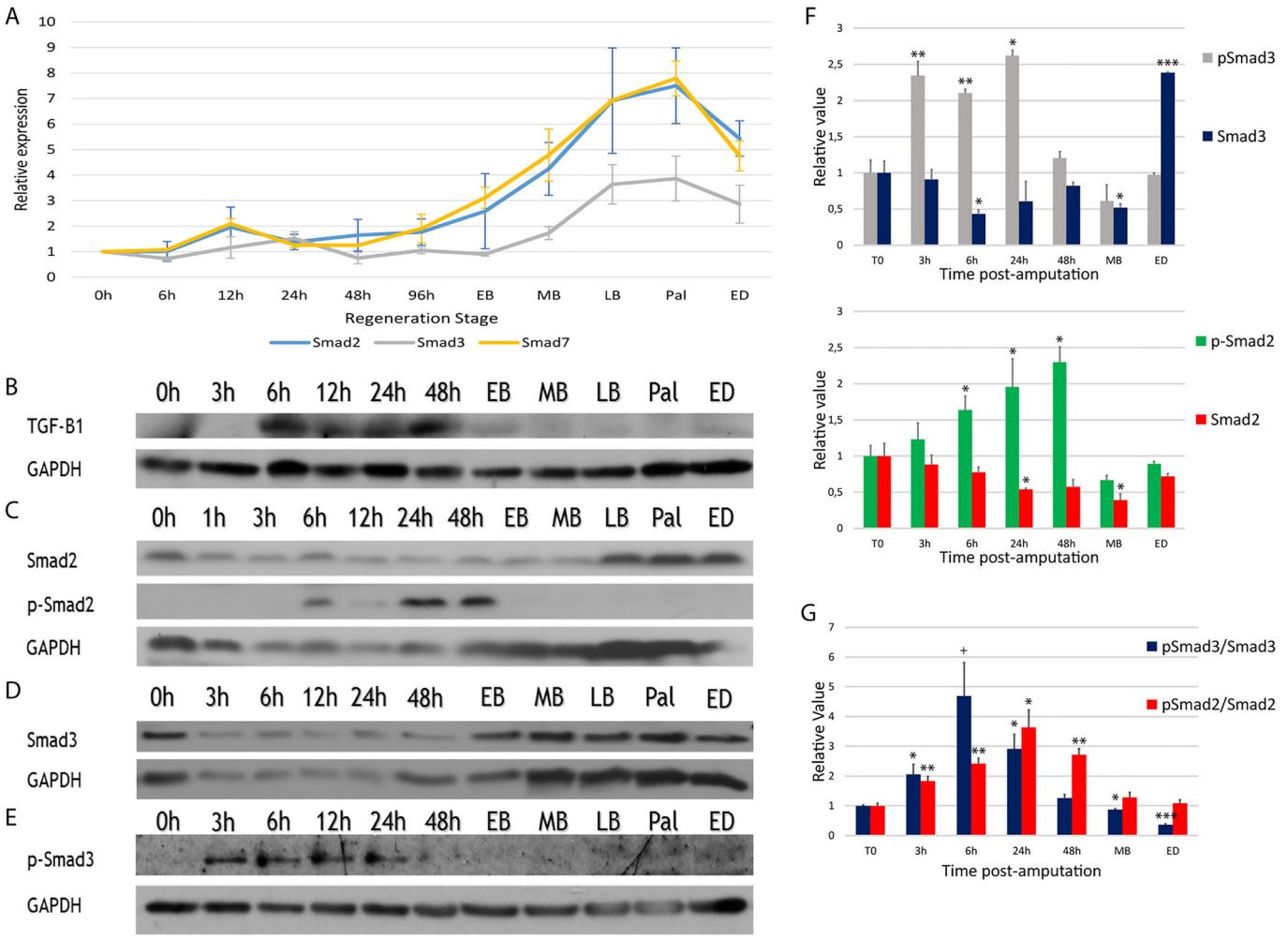

Fig. 2. Expression of Smads during normal limb regeneration. (A) Expression of *Smad2*, *Smad3* and *Smad7* RNA relative to *Gapdh*, as assessed by RT-PCR. Smads are not regulated at the RNA level during the preparation phase (0-96 h post-amputation). Expression increases for all three Smads during the redevelopment phase (EB-ED). Data show mean±s.e.m., n=3. (B-E) Western blots. (B) Expression of TGF-β1 (12.5 kDa, active form). Maximal expression is detected during the preparation phase between 6 h and 48 h. (C) Smad2 and p-Smad2 (active form). Activation is maximal between 6 h and 48 h. (D) Expression of total Smad3 protein. Levels of Smad3 are lower during the preparation phase than the redevelopment phase. (E) p-Smad3 is detected early (3 h post-amputation), earlier than observed for p-Smad2. (F) Quantification of Smad proteins (densitometric analysis from C-E) during regeneration. (G) Ratio of p-Smad over total Smad. Maximal activation of Smad3 occurs before maximal activation of Smad2. Welch's t-test was performed to compare t=0 h with each time point: ***P<0.005, **P<0.01, *P<0.05, ^{+}P<0.08. Mean±s.e.m. (normalized using GAPDH, n=4). EB, early bud; MB, medium bud; LB, late bud; Pal, palette; ED, early differentiation.

In order to clarify further the role of Smad3 in the regenerative process, we performed electroporation of wild-type and a phosphomimetic axolotl Smad3 *in vivo*. We did not observe any scarring or any effect on the regeneration process (data not shown). However, the GFP tracer rapidly disappeared when axolotl Smad3 was co-electroporated. We performed TUNEL assays and observed increased numbers of apoptotic cells (Figs S4 and S5), which would explain the disappearance of the tracer and the lack of a phenotype, since cells overexpressing Smad3 are eliminated via apoptosis.

Since limb regeneration is a complex process involving multiple cell types, we performed immunofluorescence analyses to visualize the cells that exhibit p-Smad2 and p-Smad3 during regeneration. p-Smad2 can be observed in epithelial cells and in mesenchymal cells underneath the wound epithelium in control limbs (Fig. 4B,B′; see Fig. S6 for additional time points). In SB-431542-treated limbs, p-Smad2 is very limited (Fig. 4D,D′,E, Fig. S6). Phosphorylation of Smad3 occurs mostly in epithelial cells and is enriched in the wound epithelium (Fig. 5B,B′; see Fig. S7 for additional time point). In SIS3-treated limbs, most cells are negative for p-Smad3 owing to a decrease in p-Smad3-positive cells of over 85% (Fig. 5D,D′,E, Fig. S7). The immunofluorescence results for p-Smad2 and p-Smad3 corresponded exactly to those obtained by western blot analysis, in that no immunofluorescence signal was detected at medium bud or palette stage for either protein with or without SB-431542 treatment (see Fig. S8).

All observations thus far indicate that p-Smad2 is crucial for blastema formation, whereas p-Smad3 is less important and its inhibition does not affect regeneration. This further suggests differential roles of Smad proteins during regeneration.

TGF-β target MMPs are affected by SB-431542, whereas non-target MMPs are not

TGF-β controls a variety of targets, including genes responsible for matrix remodeling. In wound healing, matrix remodeling is an important mechanism in promoting cell migration and cell proliferation. Cell migration has not been assessed in SB-431542-

Development (2016) 143, 3481-3490 doi:10.1242/dev.131466

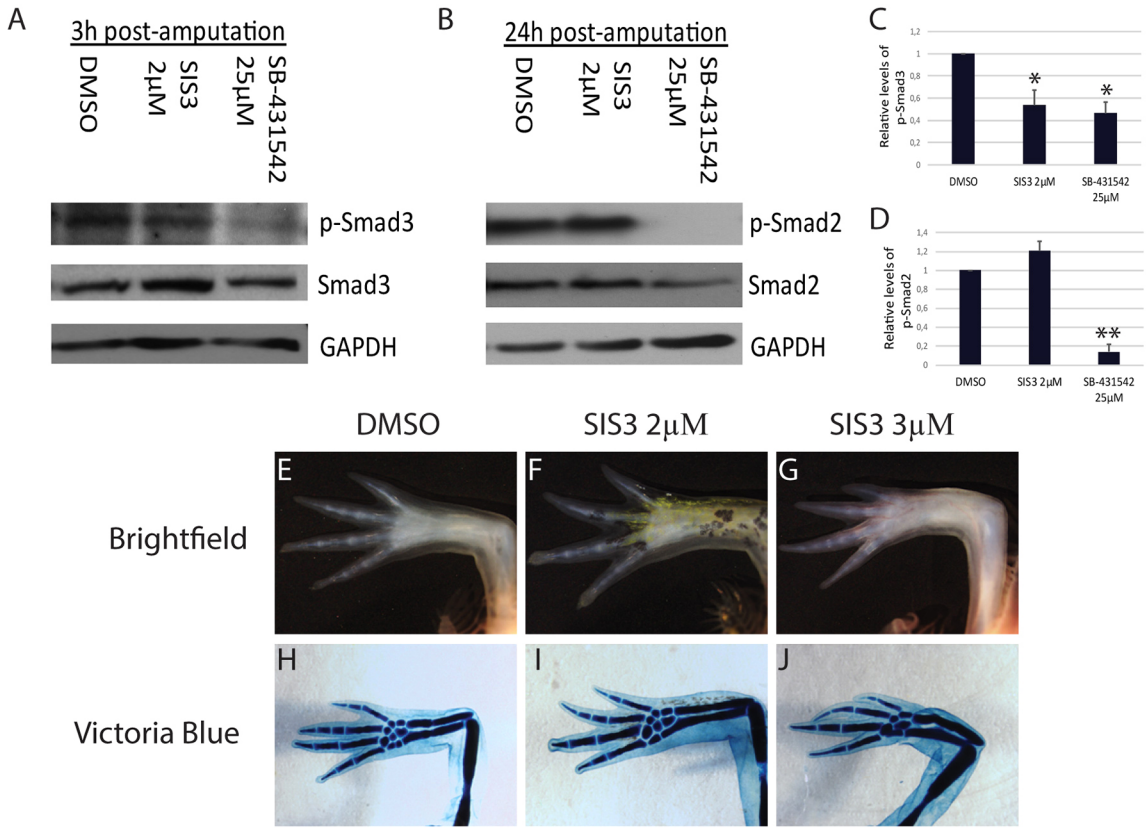

Fig. 3. Inhibition of Smad3 phosphorylation has minimal effect on limb regeneration. (A,B) Western blot. Animals were treated with 25 µM SB-431542, 2 µM SIS3, or DMSO as control. (A) Proteins were harvested 3 h post-amputation. Blot shows that p-Smad3 is reduced in SB-431542 and in SIS3 treatment conditions. (B) Proteins were harvested 24 h post-amputation. Smad2 phosphorylation is blocked at 24 h post-amputation by SB-431542 treatment only. (C) Quantification (from A) shows significant differences between DMSO and inhibitors (SIS3 and SB-431542) for p-Smad3 levels. (D) Quantification (from B) shows a significant difference between DMSO and SB-431542 but not SIS3 for p-Smad2 levels. (E-J) Ongoing SIS3 treatments with (E,H) DMSO control, (F,I) 2 µM SIS3 or (G,J) 3 µM SIS3 for 35 days. No differences can be observed in brightfield (E-G) and only minor differences can be discerned after Victoria Blue staining in SIS3-treated limbs (missing carpal or phalange in some limbs) (J). Welch's *t*-test was performed to compare protein phosphorylation under different conditions at 3 h and 24 h: $^{**}P<0.01$, $^{*}P<0.05$. Mean±s.e.m. (normalized using GAPDH, $n=3$).

treated limbs, but cellular proliferation is greatly reduced. In addition, in limbs treated with SB-431542 we do not see any cell accumulation under the wound epithelium that could result from either a lack of migration and/or proliferation (Fig. 1D). Therefore, we performed RT-PCR experiments to assess the effects of SB-431542 treatment on the expression of TGF-β1 target MMPs and compare them with other MMPs that are known not to be targets of TGF-β1. *Mmp2* and *Mmp9* are known targets of TGF-β. Their expression is augmented in cancer models (Wiercinska et al., 2011) and during regeneration (Yang and Bryant, 1994; Yang et al., 1999a). When treated with SB-431542, the expression of these two MMPs is diminished (Fig. 6A,B). This could in part explain the lack of cellular migration and proliferation observed in SB-431542-treated limbs. The expression of other MMPs (*Mmp13* and *Mmp14*) that are not TGF-β1 targets was not affected by this treatment, at least not to the same extent (Fig. 6). *Mmp14* was reduced slightly after 5 days of SB-431542 treatment, which is likely to be the result of indirect effects of TGF-β1 inhibition via p38 and Erk, since this MMP is not a canonical target of TGF-β (Kuo et al., 2009; Gomes et al., 2012).

DISCUSSION

Inhibition of TGF-β signaling with SB-431542 does not prevent wound closure but does prevent blastema formation (Fig. 1) (Levesque et al., 2007). One possible explanation is that SB-431542 treatment affects signaling between the AEC and underlying mesenchymal cells. The AEC is a permissive epithelium (Mullen et al., 1996; Christensen and Tassava, 2000; Han et al., 2001) that is essential for the regeneration process (Wallace, 1981). In mature limbs the basement membrane, which is constituted mainly of collagens, separates epithelial from mesenchymal cells, limiting their interactions. Following amputation, this structure is absent from the amputation plane and is not restored completely until the very end of the regeneration process (Neufeld and Day, 1996; Neufeld et al., 1996). Premature restoration of this structure could limit signaling between the AEC and mesenchymal cells, hence preventing blastema formation. Using collagen-specific histological staining (Picrosirius Red) and Col IV immunofluorescence we show that the basement membrane is not restored prematurely upon SB-431542 treatment. Although TGF-β1 activity is essential for blastema formation, inhibiting its signaling does not cause premature restoration of the basement membrane.

Canonical TGF-β signaling occurs via Smad2 and Smad3, which are phosphorylated by TGF-β type I receptor (ALK5). Recent studies have revealed functional differences between Smad2 and Smad3 (Piek et al., 2001; Brown et al., 2007; Ungefroren et al., 2011). Smad2 has a 30 amino acid insert in the MH1 domain that prevents direct DNA binding (Brown et al., 2007), whereas Smad3 binds to target sequences in the promoter of genes such as *Smad7* (Denissova et al., 2000). Despite its indirect DNA binding, Smad2

Development (2016) 143, 3481-3490 doi:10.1242/dev.131466

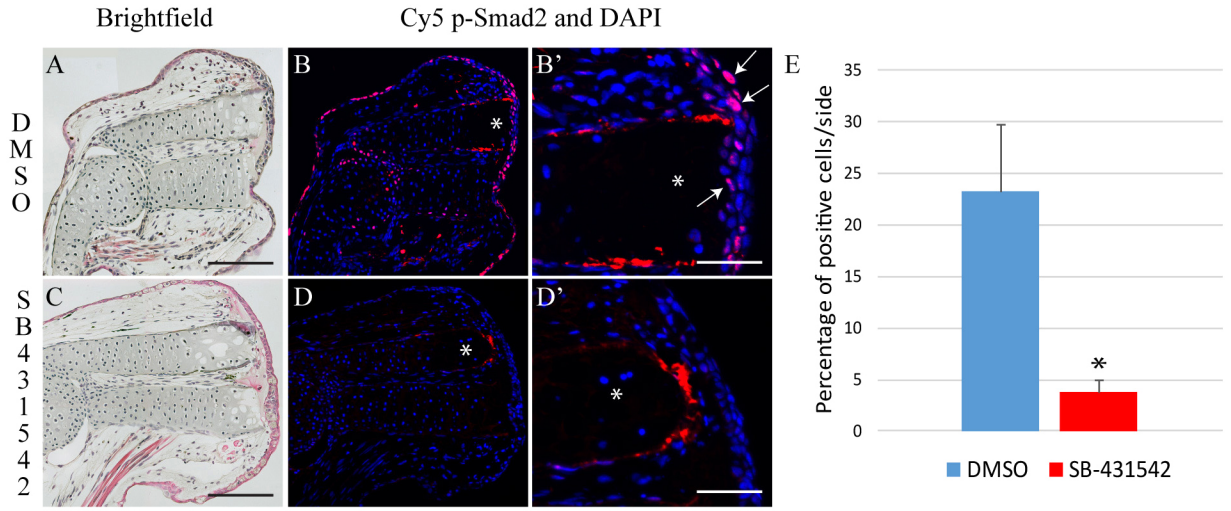

Fig. 4. SB-431542 prevents phosphorylation of Smad2 in regenerating limbs. (A-B′) Control animal treated for 24 h post-amputation with DMSO. (A) Hematoxylin and Eosin staining, brightfield image. (B) Nuclei staining (DAPI, blue) overlaid with immunofluorescence of p-Smad2 (red) shows Smad2 phosphorylation in most cells of the wound epithelium and in some underlying mesenchymal cells. (B′) Magnified view from B in the region of the asterisk. Phosphorylated proteins are often seen in the nucleus (pink, examples indicated with arrows). (C-D′) Animal treated for 24 h post-amputation with 25 µM SB-431542. (C) Hematoxylin and Eosin staining, brightfield image. (D) Overlay of DAPI and p-Smad2 immunofluorescence shows very few p-Smad2-positive cells when treated with SB-431542. (D′) Magnified view from D in the region of the asterisk. Composite images are shown in A-D. (E) Quantification (%) of cells positive for nuclear p-Smad2. Error bars indicate s.e.m. Welch's *t*-test was performed to compare protein phosphorylation levels: **P*<0.05 (*n*=5). Scale bars: 200 µm in A,C; 50 µm in B′,D′.

is associated with cellular migration and proliferation, while Smad3 is known to control the production of matrix components such as collagens, the main ECM components implicated in fibrosis/scarring (Brown et al., 2007). The axolotl Smad2 and Smad3 proteins exhibit very high identity with their human homologs, indicating that domains of interaction and functions are conserved.

The expression of *Smad2*, *Smad3* and *Smad7* mRNA was determined for all stages of regeneration. Expression of all three genes is biphasic (Fig. 2), showing low expression during the preparation phase and an increase during the redevelopment phase. These upregulation patterns during the redevelopment phase correlate with an accumulation of cells in the regenerative process (Wallace, 1981).

Expression of TGF-β1 is maximal between 6 h and 48 h, correlating with when mesenchymal cells start to migrate under the AEC, the initial step leading to blastema formation. Normally, the presence of active TGF-β1 leads to phosphorylation of Smad proteins. Our results show that p-Smad2 is maximal between 6 h and 48 h, which correlates perfectly with the presence of active TGF-β1. Smad2 phosphorylation has been described in other

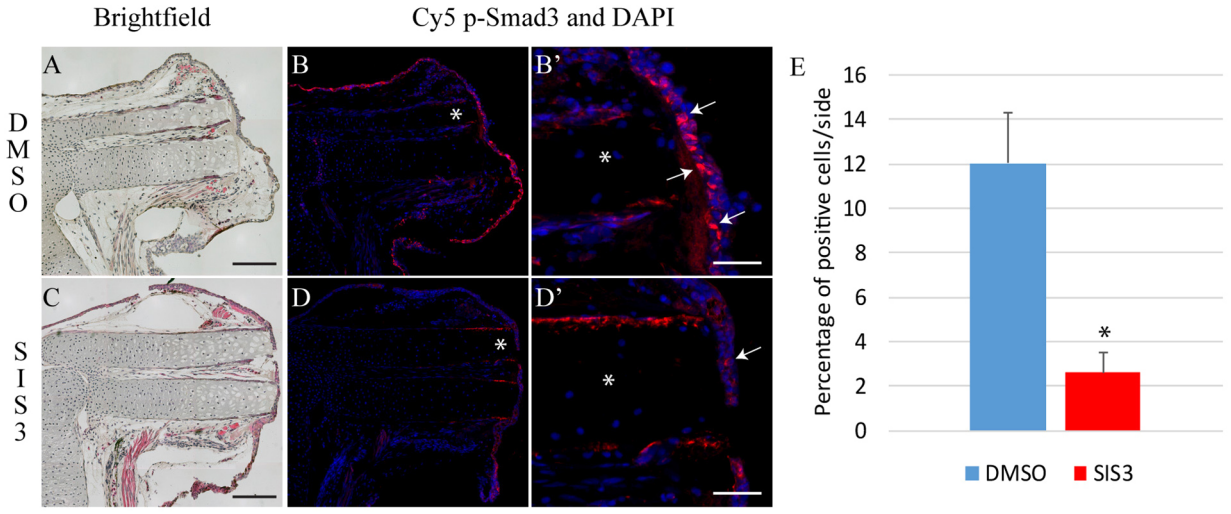

Fig. 5. SIS3 treatment reduces p-Smad3 in regenerating limbs. (A-B′) Control animal treated for 6 h post-amputation with DMSO. (A) Hematoxylin and Eosin staining, brightfield image. (B) Overlay of nuclei staining (DAPI, blue) and p-Smad3 immunofluorescence (red) shows Smad3 phosphorylation in cells of the wound epithelium. (B′) Magnified view from B in the region of the asterisk, showing that p-Smad3 is often seen in the nucleus (pink, examples indicated by arrows). (C-D′) Animal treated for 6 h post-amputation with 5 µM SIS3. (C) Hematoxylin and Eosin staining, brightfield image. (D) Overlay of nuclei staining (DAPI, blue) and p-Smad3 immunofluorescence (red) shows reduced Smad3 phosphorylation. (D′) Magnified view (in the region of the asterisk in D) showing that p-Smad3 signal is not localized in the nucleus (arrow). Composite images are shown in A-D. (E) Quantification (%) of cells positive for nuclear p-Smad3. Error bars indicate s.e.m. Welch's *t*-test was performed to compare protein phosphorylation levels: **P*<0.05 (*n*=3). Scale bars: 300 µm in A,C; 60 µm in B′,D′.

Development (2016) 143, 3481-3490 doi:10.1242/dev.131466

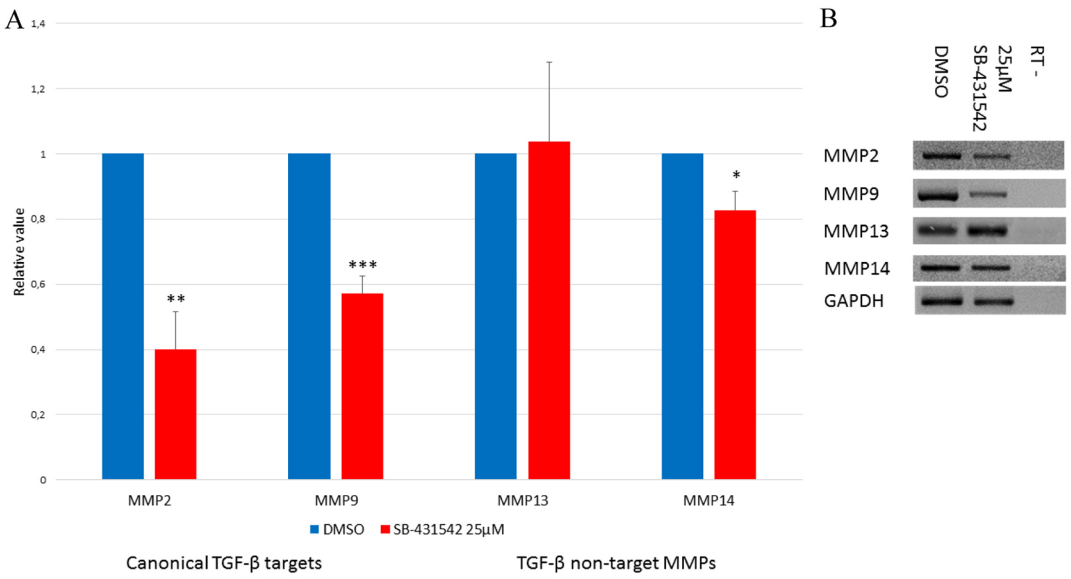

Fig. 6. SB-431542 treatment reduces expression of canonical TGF-β target MMPs. Animals were treated for 5 days post-amputation. (A) RT-PCR results. Animals were treated with DMSO (blue) or 25 µM SB-431542 (red). TGF-β target genes (*Mmp2* and *Mmp9*) are affected by SB-431542 treatment, whereas non-targets (*Mmp13*) are not affected or not very much (*Mmp14*). Welch's *t*-test was performed to compare control and treated limbs: ***P<0.005, ** P<0.01, *P<0.05 (n=5). Mean±s.e.m. (normalized using *Gapdh*). (B) Agarose gel showing expression of MMP genes and *Gapdh* after a 5-day treatment with DMSO or SB-431542. RT–, RT-PCR control without reverse transcriptase.

regenerating organisms, such as *Xenopus* (Ho and Whitman, 2008) and gecko (Gilbert et al., 2013). In both cases, p-Smad2 is associated with the wound epithelium. Similarly, our results show that p-Smad2 is located mostly in the wound epithelium. Ho and Whitman (2008) reported that p-Smad2 colocalizes with active TGF-β5 [the *Xenopus* homolog of mammalian TGFβ1 (Burt and Law, 1994)], with maximal phosphorylation at 24 h post-wounding. When TGF-β signaling is impaired with SB-431542, the wound epithelium fails to form in *Xenopus* and regeneration does not occur (Ho and Whitman, 2008). In axolotl limb regeneration, a wound epithelium is formed following SB-431542 treatment but cellular proliferation and blastema formation are abrogated (Fig. 1) (Levesque et al., 2007). These disparities are likely to be due to the very different doses of SB-431542 used: 25 µM in our study versus 100 µM in the Ho and Whitman study. We determined the optimum dose of SB-431542 for use in axolotl, such that regeneration is inhibited without preventing normal growth or affecting the health of the animal (Levesque et al., 2007). If axolotls are treated with 100 µM SB-431542 they do not survive more than 48 h (data not shown) and we deemed it toxic. It is possible that *Xenopus* tadpoles can withstand higher doses than axolotls, and if axolotls could survive at such high concentrations of SB-431542 it might well prevent wound closure as well. Gilbert et al. (2013) reported that p-Smad2 is seen throughout tail regeneration in gecko, specifically in the blastema. The authors propose that activation of Smad2 is Activin rather than TGF-β1 related. Our PCR results indicate that Activins and *Tgf-β2* are not upregulated during axolotl limb regeneration (data not shown). Therefore, the Smad2 phosphorylation observed in regenerating axolotl limbs is more likely to be due to TGF-β1 activity, and the differences observed between *Xenopus*, geckos and axolotls are likely to be species-specific characteristics.

Smad3 activation is associated with scarring in mammals. This function for Smad3 is supported by the phenotype of *Smad3* KO mice (Ashcroft et al., 1999; Flanders, 2004). p-Smad3 has also been described in zebrafish heart regeneration. Activation of Smad3 via Activin/TGF-β in zebrafish heart leads to the formation of a transient scar that is later resolved to achieve regeneration (Chablais and Jazwinska, 2012). Treatment with SB-431542 prevents phosphorylation of Smad3 and hence the heart regeneration process in zebrafish is inhibited. However, Chablais and Jazwinska (2012) did not look at p-Smad2 and they did not test Smad3-specific inhibitors, such as SIS3, to confirm that inhibition of heart regeneration was due solely to the loss of p-Smad3. In axolotl limb regeneration, scar formation is never observed (Levesque et al., 2007, 2010; Denis et al., 2013). We observe low levels of p-Smad3 very early post-amputation (Figs 2 and 5). In addition, specifically inhibiting Smad3 phosphorylation using SIS3 or Naringenin does not affect regeneration. Finally, overexpression of Smad3 does not impair limb regeneration nor does it cause scarring. This is largely due to the fact that these overexpressing cells are eliminated via apoptosis (Figs S4 and S5). p-Smad3 is likely to have limited activity in axolotl limb regeneration (it is detected at very low levels and there is no effect when inhibited) during the preparation phase. Our study did look at the levels of p-Smad2 in animals treated with SIS3 and Naringenin. The results showed clearly that these inhibitors had no effect on p-Smad2 levels, although they significantly inhibited Smad3 phosphorylation.

None of the aforementioned studies compared the expression and activation of Smad2 and Smad3 (Ho and Whitman, 2008; Chablais and Jazwinska, 2012; Gilbert et al., 2013). Multiple studies have shown that these two proteins have different functions (Piek et al., 2001; Petersen et al., 2010; Ungefroren et al., 2011). Our results show that in regenerating axolotl limbs there is a differential activation of Smad2 and Smad3. Smad3 is active very early and at low levels compared with p-Smad2. Specific inhibitors of Smad3 phosphorylation, SIS3 (50% inhibition as assessed by western blot and over 80% by immunofluorescence) and Naringenin, significantly reduce the level of p-Smad3 but have no effect on regeneration. Overexpression of Smad3 does not affect regeneration either. p-Smad2 is correlated to the active form of TGF-β1 and is clearly inhibited by treatment with SB-431542. Smad2 inhibition is

Development (2016) 143, 3481-3490 doi:10.1242/dev.131466

strongly correlated with a lack of cellular proliferation and the absence of blastema formation. Also, *Smad7*, a known Smad3 target gene, does not show any increase in expression at the time points when p-Smad3 is detected, supporting the idea that Smad3 activation is not very strong/important during the early phase of limb regeneration.

TGF-β1 is known to regulate MMPs (Kahari and Saarialho-Kere, 1997), which are essential during wound healing for matrix remodeling and proper cell migration. In normal axolotl wound healing and limb regeneration, the expression of MMP2 and MMP9 has been described (Yang and Bryant, 1994; Yang et al., 1999a; Seifert et al., 2012). MMPs are also essential for regeneration, since the broad spectrum inhibitor of MMPs, GM6001, prevents blastema formation and regeneration (Vinarsky et al., 2005). We show that following treatment with the TGF-β inhibitor SB-431542, MMP2 and MMP9 are significantly diminished. Interestingly, it was reported that MMP2 is most likely regulated by Smad2 (Piek et al., 2001; Meng et al., 2010). Other MMPs, such as MMP13 and MMP14, are not known to be regulated by the TGF-β canonical signaling pathway (Johansson et al., 2000; Takahashi et al., 2002; Leivonen et al., 2006) and are unaffected (MMP13) or only slightly affected (MMP14) by SB-431542 treatment. Consequently, inhibition of Smad2 activation correlates with the diminished expression of target MMPs. These matrix proteases might be essential in providing the proper environment for mesenchymal cells to migrate, similar to what has been described in cancer invasion (Wiercinska et al., 2011). Other MMPs, such as MMP13 and MMP14, might be employed in other processes such as wound closure or to prevent the basal lamina from reforming by preventing the deposition of Col IV, which is degraded by MMP13 (Knauper et al., 1997; Ravanti et al., 1999), independently of the TGF-β canonical pathway.

This study is the first to examine the activation of the TGF-β canonical signaling mediators Smad2 and Smad3 in the context of epimorphic regeneration. It is also the first study to demonstrate that Smad2 and Smad3 are differentially regulated during regeneration and that Smad2 activation is essential for axolotl limb regeneration. The level of p-Smad3 is low compared with that of p-Smad2, indicating that limb regeneration is controlled by a differential activation of Smad proteins. Specific inhibition or overexpression of Smad3 does not affect the regeneration process in axolotl. Treatment with SB-431542 greatly inhibits the phosphorylation of Smad2 and, consequently, inhibits regeneration. Treatment with Smad3-specific inhibitors has no effect on regeneration, even though they achieved the same level of inhibition as SB-431542. These results suggest that inhibition of the canonical TGF-β pathway blocks regeneration by preventing the activation of Smad2.

MATERIALS AND METHODS

Animal maintenance and treatments

Axolotls (*Ambystoma mexicanum*) were purchased from the Ambystoma Genetic Stock Center (Lexington, KY, USA) and maintained as described (Levesque et al., 2007). SB-431542 and SIS3 were purchased from Sigma-Aldrich. 10 mM stock solutions were prepared in DMSO (Sigma-Aldrich). After amputation, 4 cm animals were kept in 5 ml and 6 cm animals were kept in 10 ml 20% Holtfreter's solution containing 25 µM SB-431542. SIS3 treatments were at 2, 3 or 5 µM. Control animals were treated with DMSO (same volumes as for SB-431542 and SIS3 compounds). Solutions were changed daily. Animal care and experiments were performed in accordance with Université de Montréal Animal Care Committee guidelines.

Production of antibody against axolotl p-Smad3

A peptide corresponding to the phosphorylated C-terminus of axolotl Smad3 (CGMGTPSLRCSpSVpS) was synthesized (Biomatik) with the phospho-serine residues corresponding to positions 423 and 425. Peptide was diluted in sterile PBS at 10 mg/ml. KLH (ThermoFisher Scientific, 77606) was diluted in sterile water at 10 mg/ml for conjugation with the peptide. Peptide and KLH solutions were mixed and incubated 2 h at room temperature then stored at −20°C until use. Prior to injection, peptide-KLH solution was diluted (400 µg/ml peptide) in sterile PBS. Freund's incomplete adjuvant (Sigma-Aldrich) was added to a final peptide concentration of 200 µg/ml. Five 25-day-old BALB/c mice were injected subcutaneously on the back with this mixture. Booster shots were administered at 14 days and 28 days. Serum was collected prior to first injection (pre-serum) and after 10 weeks. Serum was collected in a microtainer (BD, 365956) and separated following the manufacturer's protocol. Western blot analyses were performed to assess the presence of antibodies against axolotl p-Smad3 in the serum.

RT-PCR

RNA extraction and RT-PCR were performed as described (Levesque et al., 2007); primers are listed in Table S1. For each non-treated regeneration stage, two animals of 6 cm (four blastemas) were pooled per preparation for a total of six animals (n=3 independent replicates). To measure the effect of SB-431542 on TGF-β1 target genes, animals were treated with 25 µM SB-431542 or DMSO for 5 days following amputation, two animals of 6 cm (four blastemas) were pooled per preparation for a total of eight animals (n=4 independent replicates). For quantification, densitometric analysis was performed using the AlphaEaseFC (Fluor-Chem 8900) program. Gene expression was normalized using *Gapdh*, which has been demonstrated to be the most appropriate standard during limb regeneration in urodeles (Vascotto et al., 2005). Relative values are represented compared with t=0 h.

Western blotting

For each non-treated regeneration stage, two animals of 6 cm (four blastemas) were used per preparation for a total of eight animals (n=4 independent replicates). To measure the effects of SB-431542 and SIS3 on phosphorylation of Smad2 and Smad3, animals were treated for 3 h or for 24 h following amputation with 25 µM SB-431542, 2 µM SIS3 or DMSO as a control for the carrier of the drugs. Proteins were extracted by sonication in Laemmli buffer containing 50 mM NaF. Proteins were quantified using EZQ Reagent (Invitrogen, R33200) following the manufacturer's protocol. 30 µg protein was loaded per lane on 10% SDS-PAGE gels. Proteins were transferred electrophoretically onto Immobilon PVDF membranes (Millipore, IPVH00010). Antibodies and blotting conditions are described in Table S2. For quantification, densitometric analysis was performed using Adobe Photoshop CS4. Protein expression was normalized using GAPDH and relative values compared with t=0 h (i.e. unamputated control) are presented.

Picrosirius Red staining

Following treatments with SB-431542 or DMSO, animals were fixed overnight in 4% paraformaldehyde in 0.7× PBS at 4°C. The following day, tissues were rinsed thoroughly with 0.7× PBS and embedded in paraffin. To assess the presence of the basement membrane, 10 µm sections were rehydrated then stained with Weigert's Hematoxylin for 10 min, rinsed with running tap water and then stained with Picrosirius Red (ThermoFisher Scientific, B21693) for 1 h. Slides were dehydrated and mounted using Permount (Fisher Scientific). Polarized light was used to visualize collagen fibers. Slides were visualized with an Axiophot 506747 microscope (Zeiss).

Victoria Blue cartilage staining

Following treatments with SIS3 or DMSO, limbs were stained using Victoria Blue (Sigma-Aldrich, V-0753) to verify cartilage formation as previously described (Hutchison et al., 2007). Limbs were fixed in alcoholic Bouin's solution for 24 h, then rinsed several times with 70% ethanol. Limbs were rinsed multiple times with 3.5% NH_4OH for 24 h and then treated with acid alcohol (70% ethanol with 0.4% HCl) for 2 h. Specimens were stained with 1% Victoria Blue for 2 h and then rinsed with 70% ethanol. Limbs were gradually dehydrated to 100% ethanol, then cleared and stored in methyl salicylate.

Apoptosis

Apoptosis was assessed by Acridine Orange/ethidium bromide staining or by TUNEL assay following injection/electroporation (see Table S3) as described in the supplementary Materials and Methods.

Immunofluorescence enhanced with tyramide

Sections of treated limbs were rehydrated as previously described (Levesque et al., 2007). Epitope retrieval was performed (1% SDS for 5 min at room temperature for p-Smad3; and citric acid for 20 min at 95°C for Col IV). Slides were blocked using 2% BSA in TBS-T (Tris-buffered saline with 0.1% Tween 20) for 1 h at room temperature for p-Smad2 and p-Smad3 or with Power Block 1× (Hk085.5K, BioGenex) for 15 min at room temperature for Col IV. Primary antibodies anti-p-Smad2 (3101, Cell Signaling; 1/400) and anti-p-Smad3 (homemade mouse antibody; 1/500) were diluted in blocking solution and anti-Col IV (ab6586, Abcam; 1/500) in PBS and incubated overnight at 4°C. Anti-rabbit-HRP and anti-mouse-HRP (170-6515 and 170-6516, Bio-Rad; 1/400) secondary antibodies were diluted in blocking solution for p-Smads or PBS for Col IV and incubated at room temperature for 45 min. Tyramide (Biotium, 92175) was diluted in TBS with 0.0015% H_2O_2 to 11.6 µM then incubated at room temperature for 8 min. All slides were mounted with ProLong Gold antifade reagent containing DAPI (Invitrogen, 36931). Slides were visualized with a Zeiss Axio Imager M2 optical microscope. The software used was Zeiss Zen 2 Pro Blue Edition with a Tile Module. All images were verified using the range indicator of the software to ensure that they were not saturated. The images were saved as tif files and then imported into Photoshop CS4 to adjust the rotation and to crop to be mounted into a multipanel figure using Adobe Illustrator CS4.

Statistical analysis

Cell counts were performed using ImageJ. Statistical analyses were achieved using Welch's *t*-test, which corrects biases due to an unequal number of samples and/or variances between the different groups (Scherrer, 2007). Values are presented as mean±s.e.m.

Acknowledgements

Special thanks to Dr Ken Finnson for help with antibodies; Dr Mathieu Lévesque for help with western blots and detection of TGF-β1; the laboratory of Dr Antonio Nanci for help with their microscopes; and Dr Elly Tanaka and Dr Prayag Murawala of the Center for Regenerative Therapies in Dresden for constructive input.

Competing interests

The authors declare no competing or financial interests.

Author contributions

J.-F.D. performed 80% of the experiments and helped design, analyze and interpret the data and co-wrote the manuscript. F.S. helped with some of the animal treatments, protein preparation and RT-PCR experiments and helped with the writing of the manuscript. S.G. cloned *Smad2* and *Smad3*. E.V. helped with protein and RNA preparation, TUNEL assay and animal husbandry. A.P. helped interpret some of the results and her lab provided antibodies for some of the western blots. S.R. designed and supervised the project, helped analyze and interpret the data and co-wrote the manuscript.

Funding

This research is supported by a grant from the Canadian Institutes of Health Research [MOP: 111013] to S.R. J.-F.D. is supported by a PhD scholarship award from the Réseau de Recherche en Santé Buccodentaire et Osseuse (RSBO).

Data availability

cDNA sequences for axolotl *Smad2* and *Smad3* are available at GenBank under accessions KT383019 and KT383020.

Supplementary information

Supplementary information available online at
http://dev.biologists.org/lookup/doi/10.1242/dev.131466.supplemental

References

Ashcroft, G. S. and Roberts, A. B. (2000). Loss of Smad3 modulates wound healing. *Cytokine Growth Factor Rev.* **11**, 125-131.

Ashcroft, G. S., Yang, X., Glick, A. B., Weinstein, M., Letterio, J. L., Mizel, D. E., Anzano, M., Greenwell-Wild, T., Wahl, S. M., Deng, C. et al. (1999). Mice lacking Smad3 show accelerated wound healing and an impaired local inflammatory response. *Nat. Cell Biol.* **1**, 260-266.

Attisano, L. and Wrana, J. L. (2002). Signal transduction by the TGF-beta superfamily. *Science* **296**, 1646-1647.

Blavier, L., Lazaryev, A., Groffen, J., Heisterkamp, N., DeClerck, Y. A. and Kaartinen, V. (2001). TGF-beta3-induced palatogenesis requires matrix metalloproteinases. *Mol. Biol. Cell* **12**, 1457-1466.

Braun, L., Mead, J. E., Panzica, M., Mikumo, R., Bell, G. I. and Fausto, N. (1988). Transforming growth factor beta mRNA increases during liver regeneration: a possible paracrine mechanism of growth regulation. *Proc. Natl. Acad. Sci. USA* **85**, 1539-1543.

Brown, K. A., Pietenpol, J. A. and Moses, H. L. (2007). A tale of two proteins: differential roles and regulation of Smad2 and Smad3 in TGF-beta signaling. *J. Cell. Biochem.* **101**, 9-33.

Burt, D. W. and Law, A. S. (1994). Evolution of the transforming growth factor-beta superfamily. *Prog. Growth Factor Res.* **5**, 99-118.

Chablais, F. and Jazwinska, A. (2012). The regenerative capacity of the zebrafish heart is dependent on TGFbeta signaling. *Development* **139**, 1921-1930.

Christensen, R. N. and Tassava, R. A. (2000). Apical epithelial cap morphology and fibronectin gene expression in regenerating axolotl limbs. *Dev. Dyn.* **217**, 216-224.

Datto, M. and Wang, X.-F. (2000). The Smads: transcriptional regulation and mouse models. *Cytokine Growth Factor Rev.* **11**, 37-48.

Datto, M. B., Frederick, J. P., Pan, L., Borton, A. J., Zhuang, Y. and Wang, X.-F. (1999). Targeted disruption of Smad3 reveals an essential role in transforming growth factor beta-mediated signal transduction. *Mol. Cell. Biol.* **19**, 2495-2504.

Denis, J.-F., Levesque, M., Tran, S. D., Camarda, A.-J. and Roy, S. (2013). Axolotl as a model to study scarless wound healing in vertebrates: role of the transforming growth factor beta signaling pathway. *Adv. Wound Care* **2**, 250-260.

Denissova, N. G., Pouponnot, C., Long, J., He, D. and Liu, F. (2000). Transforming growth factor beta -inducible independent binding of SMAD to the Smad7 promoter. *Proc. Natl. Acad. Sci. USA* **97**, 6397-6402.

Derynck, R. and Zhang, Y. E. (2003). Smad-dependent and Smad-independent pathways in TGF-beta family signalling. *Nature* **425**, 577-584.

Falanga, V., Schrayer, D., Cha, J., Butmarc, J., Carson, P., Roberts, A. B. and Kim, S.-J. (2004). Full-thickness wounding of the mouse tail as a model for delayed wound healing: accelerated wound closure in Smad3 knock-out mice. *Wound Repair Regen.* **12**, 320-326.

Flanders, K. C. (2004). Smad3 as a mediator of the fibrotic response. *Int. J. Exp. Pathol.* **85**, 47-64.

Flanders, K. C., Major, C. D., Arabshahi, A., Aburime, E. E., Okada, M. H., Fujii, M., Blalock, T. D., Schultz, G. S., Sowers, A., Anzano, M. A. et al. (2003). Interference with transforming growth factor-beta/Smad3 signaling results in accelerated healing of wounds in previously irradiated skin. *Am. J. Pathol.* **163**, 2247-2257.

Gabbiani, G. (2003). The myofibroblast in wound healing and fibrocontractive diseases. *J. Pathol.* **200**, 500-503.

Gardiner, D. M., Carlson, M. R. J. and Roy, S. (1999). Towards a functional analysis of limb regeneration. *Semin. Cell Dev. Biol.* **10**, 385-393.

Gilbert, R. W. D., Vickaryous, M. K. and Viloria-Petit, A. M. (2013). Characterization of TGFbeta signaling during tail regeneration in the leopard Gecko (Eublepharis macularius). *Dev. Dyn.* **242**, 886-896.

Godwin, J. W., Pinto, A. R. and Rosenthal, N. A. (2013). Macrophages are required for adult salamander limb regeneration. *Proc. Natl. Acad. Sci. USA* **110**, 9415-9420.

Gomes, L. R., Terra, L. F., Wailemann, R. A. M., Labriola, L. and Sogayar, M. C. (2012). TGF-beta1 modulates the homeostasis between MMPs and MMP inhibitors through p38 MAPK and ERK1/2 in highly invasive breast cancer cells. *BMC Cancer* **12**, 26.

Han, M.-J., An, J.-Y. and Kim, W.-S. (2001). Expression patterns of Fgf-8 during development and limb regeneration of the axolotl. *Dev. Dyn.* **220**, 40-48.

Han, M., Yang, X., Taylor, G., Burdsal, C. A., Anderson, R. A. and Muneoka, K. (2005). Limb regeneration in higher vertebrates: developing a roadmap. *Anat. Rec. B New Anatomist* **287B**, 14-24.

Ho, D. M. and Whitman, M. (2008). TGF-beta signaling is required for multiple processes during Xenopus tail regeneration. *Dev. Biol.* **315**, 203-216.

Hutchison, C., Pilote, M. and Roy, S. (2007). The axolotl limb: a model for bone development, regeneration and fracture healing. *Bone* **40**, 45-56.

Inman, G. J., Nicolas, F. J., Callahan, J. F., Harling, J. D., Gaster, L. M., Reith, A. D., Laping, N. J. and Hill, C. S. (2002). SB-431542 is a potent and specific inhibitor of transforming growth factor-beta superfamily type I activin receptor-like kinase (ALK) receptors ALK4, ALK5, and ALK7. *Mol. Pharmacol.* **62**, 65-74.

Iten, L. E. and Bryant, S. V. (1973). Forelimb regeneration from different levels of amputation in the newt, Notophthalmus viridescens. *Wilhelm Roux Archiv.* **173**, 263-282.

Johansson, N., Ala-aho, R., Uitto, V., Grenman, R., Fusenig, N. E., Lopez-Otin, C. and Kahari, V. M. (2000). Expression of collagenase-3 (MMP-13) and

collagenase-1 (MMP-1) by transformed keratinocytes is dependent on the activity of p38 mitogen-activated protein kinase. *J. Cell Sci.* **113**, 227-235.
Junqueira, L. C. U., Cossermelli, W. and Brentani, R. (1978). Differential staining of collagens type I, II and III by Sirius Red and polarization microscopy. *Arch. Histol. Jpn.* **41**, 267-274.
Junqueira, L. C. U., Bignolas, G. and Brentani, R. R. (1979). Picrosirius staining plus polarization microscopy, a specific method for collagen detection in tissue sections. *Histochem. J.* **11**, 447-455.
Kahari, V.-M. and Saarialho-Kere, U. (1997). Matrix metalloproteinases in skin. *Exp. Dermatol.* **6**, 199-213.
Kiraly, K., Hyttinen, M. M., Lapvetelainen, T., Elo, M., Kiviranta, I., Dobai, J., Modis, L., Helminen, H. J. and Arokoski, J. P. A. (1997). Specimen preparation and quantification of collagen birefringence in unstained sections of articular cartilage using image analysis and polarizing light microscopy. *Histochem. J.* **29**, 317-327.
Knauper, V., Cowell, S., Smith, B., Lopez-Otin, C., O'Shea, M., Morris, H., Zardi, L. and Murphy, G. (1997). The role of the C-terminal domain of human collagenase-3 (MMP-13) in the activation of procollagenase-3, substrate specificity, and tissue inhibitor of metalloproteinase interaction. *J. Biol. Chem.* **272**, 7608-7616.
Kuhn, K. (1995). Basement membrane (type IV) collagen. *Matrix Biol.* **14**, 439-445.
Kuo, Y.-C., Su, C.-H., Liu, C.-Y., Chen, T.-H., Chen, C.-P. and Wang, H.-S. (2009). Transforming growth factor-beta induces CD44 cleavage that promotes migration of MDA-MB-435s cells through the up-regulation of membrane type 1-matrix metalloproteinase. *Int. J. Cancer* **124**, 2568-2576.
Leivonen, S.-K., Ala-Aho, R., Koli, K., Grenman, R., Peltonen, J. and Kahari, V.-M. (2006). Activation of Smad signaling enhances collagenase-3 (MMP-13) expression and invasion of head and neck squamous carcinoma cells. *Oncogene* **25**, 2588-2600.
Levesque, M., Gatien, S., Finnson, K., Desmeules, S., Villiard, E., Pilote, M., Philip, A. and Roy, S. (2007). Transforming growth factor: beta signaling is essential for limb regeneration in axolotls. *PLoS ONE* **2**, e1227.
Levesque, M., Villiard, E. and Roy, S. (2010). Skin wound healing in axolotls: a scarless process. *J. Exp. Zool. B Mol. Dev. Evol.* **314B**, 684-697.
Massague, J. (2000). How cells read TGF-beta signals. *Nat. Rev. Mol. Cell Biol.* **1**, 169-178.
Massague, J. and Chen, Y. G. (2000). Controlling TGF-beta signaling. *Genes Dev.* **14**, 627-644.
Massague, J., Seoane, J. and Wotton, D. (2005). Smad transcription factors. *Genes Dev.* **19**, 2783-2810.
Meng, X. M., Huang, X. R., Chung, A. C. K., Qin, W., Shao, X., Igarashi, P., Ju, W., Bottinger, E. P. and Lan, H. Y. (2010). Smad2 protects against TGF-beta/Smad3-mediated renal fibrosis. *J. Am. Soc. Nephrol.* **21**, 1477-1487.
Mu, Y., Gudey, S. K. and Landstrom, M. (2012). Non-Smad signaling pathways. *Cell Tissue Res.* **347**, 11-20.
Mullen, L., Torok, M. A., Bryant, S. V. and Gardiner, D. M. (1996). Nerve dependency of regeneration: role of *Dlx* and FGF signaling in amphibian limb regeneration. *Development* **122**, 3487-3497.
Nakao, A., Imamura, T., Souchelnytskyi, S., Kawabata, M., Ishisaki, A., Oeda, E., Tamaki, K., Hanai, J.-I., Heldin, C.-H., Miyazono, K. et al. (1997). TGF-beta receptor-mediated signalling through Smad2, Smad3 and Smad4. *EMBO J.* **16**, 5353-5362.
Neufeld, D. A. and Aulthouse, A. L. (1986). Association of mesenchyme with attenuated basement membranes during morphogenetic stages of newt limb regeneration. *Am. J. Anat.* **176**, 411-421.
Neufeld, D. A. and Day, F. A. (1996). Perspective: a suggested role for basement membrane structures during newt limb regeneration. *Anat. Rec.* **246**, 155-161.
Neufeld, D. A., Day, F. A. and Settles, H. E. (1996). Stabilizing role of the basement membrane and dermal fibers during newt limb regeneration. *Anat. Rec.* **245**, 122-127.
Nomura, M. and Li, E. (1998). Smad2 role in mesoderm formation, left-right patterning and craniofacial development. *Nature* **393**, 786-790.
Overall, C. M., Wrana, J. L. and Sodek, J. (1991). Transcriptional and post-transcriptional regulation of 72-kDa gelatinase/type IV collagenase by transforming growth factor-beta 1 in human fibroblasts. Comparisons with collagenase and tissue inhibitor of matrix metalloproteinase gene expression. *J. Biol. Chem.* **266**, 14064-14071.
Petersen, M., Pardali, E., van der Horst, G., Cheung, H., van den Hoogen, C., van der Pluijm, G. and Ten Dijke, P. (2010). Smad2 and Smad3 have opposing roles in breast cancer bone metastasis by differentially affecting tumor angiogenesis. *Oncogene* **29**, 1351-1361.
Piek, E., Ju, W. J., Heyer, J., Escalante-Alcalde, D., Stewart, C. L., Weinstein, M., Deng, C., Kucherlapati, R., Bottinger, E. P. and Roberts, A. B. (2001). Functional characterization of transforming growth factor beta signaling in Smad2- and Smad3-deficient fibroblasts. *J. Biol. Chem.* **276**, 19945-19953.
Poschl, E., Schlotzer-Schrehardt, U., Brachvogel, B., Saito, K., Ninomiya, Y. and Mayer, U. (2004). Collagen IV is essential for basement membrane stability but dispensable for initiation of its assembly during early development. *Development* **131**, 1619-1628.
Ravanti, L., Heino, J., Lopez-Otin, C. and Kahari, V.-M. (1999). Induction of collagenase-3 (MMP-13) expression in human skin fibroblasts by three-dimensional collagen is mediated by p38 mitogen-activated protein kinase. *J. Biol. Chem.* **274**, 2446-2455.
Roy, S. and Lévesque, M. (2006). Limb regeneration in axolotl: is it superhealing? *TSW Dev. Embryol.* **6**, 12-25.
Scherrer, B. (2007). *Biostatistique*. Montréal: Chenelière Education.
Sehgal, I. and Thompson, T. C. (1999). Novel regulation of type IV collagenase (matrix metalloproteinase-9 and -2) activities by transforming growth factor-beta1 in human prostate cancer cell lines. *Mol. Biol. Cell* **10**, 407-416.
Seifert, A. W., Monaghan, J. R., Voss, S. R. and Maden, M. (2012). Skin regeneration in adult axolotls: a blueprint for scar-free healing in vertebrates. *PLoS ONE* **7**, e32875.
Sirard, C., de la Pompa, J. L., Elia, A., Itie, A., Mirtsos, C., Cheung, A., Hahn, S., Wakeham, A., Schwartz, L., Kern, S. E. et al. (1998). The tumor suppressor gene Smad4/Dpc4 is required for gastrulation and later for anterior development of the mouse embryo. *Genes Dev.* **12**, 107-119.
Smith, J. J. and Voss, S. R. (2006). Gene order data from a model amphibian (Ambystoma): new perspectives on vertebrate genome structure and evolution. *BMC Genomics* **7**, 219.
Takahashi, M., Tsunoda, T., Seiki, M., Nakamura, Y. and Furukawa, Y. (2002). Identification of membrane-type matrix metalloproteinase-1 as a target of the beta-catenin/Tcf4 complex in human colorectal cancers. *Oncogene* **21**, 5861-5867.
Tank, P. W., Carlson, B. M. and Connelly, T. G. (1976). A staging system for forelimb regeneration in the axolotl, *Ambystoma mexicanum*. *J. Morphol.* **150**, 117-128.
Ungefroren, H., Groth, S., Sebens, S., Lehnert, H., Gieseler, F. and Fandrich, F. (2011). Differential roles of Smad2 and Smad3 in the regulation of TGF-beta1-mediated growth inhibition and cell migration in pancreatic ductal adenocarcinoma cells: control by Rac1. *Mol. Cancer* **10**, 67.
Vascotto, S. G., Beug, S., Liversage, R. A. and Tsilfidis, C. (2005). Nvbeta-actin and NvGAPDH as normalization factors for gene expression analysis in limb regenerates and cultured blastema cells of the adult newt, Notophthalmus viridescens. *Int. J. Dev. Biol.* **49**, 833-842.
Vinarsky, V., Atkinson, D. L., Stevenson, T. J., Keating, M. T. and Odelberg, S. J. (2005). Normal newt limb regeneration requires matrix metalloproteinase function. *Dev. Biol.* **279**, 86-98.
Waldrip, W. R., Bikoff, E. K., Hoodless, P. A., Wrana, J. L. and Robertson, E. J. (1998). Smad2 signaling in extraembryonic tissues determines anterior-posterior polarity of the early mouse embryo. *Cell* **92**, 797-808.
Wallace, H. (1981). *Vertebrate Limb Regeneration*. Chichester: John Wiley and Sons.
Weinstein, M., Yang, X., Li, C., Xu, X., Gotay, J. and Deng, C.-X. (1998). Failure of egg cylinder elongation and mesoderm induction in mouse embryos lacking the tumor suppressor smad2. *Proc. Natl. Acad. Sci. USA* **95**, 9378-9383.
Wiercinska, E., Naber, H. P. H., Pardali, E., van der Pluijm, G., van Dam, H. and ten Dijke, P. (2011). The TGF-beta/Smad pathway induces breast cancer cell invasion through the up-regulation of matrix metalloproteinase 2 and 9 in a spheroid invasion model system. *Breast Cancer Res. Treat.* **128**, 657-666.
Wrana, J. L. and Attisano, L. (2000). The Smad pathway. *Cytokine Growth Factor Rev.* **11**, 5-13.
Yang, E. V. and Bryant, S. V. (1994). Developmental regulation of a matrix metalloproteinase during regeneration of axolotl appendages. *Dev. Biol.* **166**, 696-703.
Yang, E. V., Gardiner, D. M., Carlson, M. R. J., Nugas, C. A. and Bryant, S. V. (1999a). Expression of Mmp-9 and related matrix metalloproteinase genes during axolotl limb regeneration. *Dev. Dyn.* **216**, 2-9.
Yang, X., Letterio, J. J., Lechleider, R. J., Chen, L., Hayman, R., Gu, H., Roberts, A. B. and Deng, C. (1999b). Targeted disruption of SMAD3 results in impaired mucosal immunity and diminished T cell responsiveness to TGF-beta. *EMBO J.* **18**, 1280-1291.
Zentella, A. and Massague, J. (1992). Transforming growth factor beta induces myoblast differentiation in the presence of mitogens. *Proc. Natl. Acad. Sci. USA* **89**, 5176-5180.
Zhang, Y. E. (2009). Non-Smad pathways in TGF-beta signaling. *Cell Res.* **19**, 128-139.
Zhang, Y., Feng, X.-H., Wu, R.-Y. and Derynck, R. (1996). Receptor-associated Mad homologues synergize as effectors of the TGF-beta response. *Nature* **383**, 168-172.
Zhao, Y. (1999). Transforming growth factor-beta (TGF-beta) type I and type II receptors are both required for TGF-beta-mediated extracellular matrix production in lung fibroblasts. *Mol. Cell. Endocrinol.* **150**, 91-97.
Zhu, Y., Richardson, J. A., Parada, L. F. and Graff, J. M. (1998). Smad3 mutant mice develop metastatic colorectal cancer. *Cell* **94**, 703-714.

Supplementary Materials and Methods:

Cloning of Axolotl Smad2, Smad3 and Smad7

Partial axolotl Smad2, Smad3 and Smad7 cDNA were obtained from axolotl larvae total RNA by RT-PCR. The cDNAs were amplified with primers (see sup. table1) designed from human cDNA sequences. The full length Smad2, Smad3 and partial Smad7 cDNA were subsequently obtained by screening an axolotl cDNA library (Stratagene, CA, USA), following the manufacturer's instructions and using the RT-PCR fragments as probes radioactively labeled with α^{32}P-dCTP (Perkin Elmer, MA, USA).

Acridine Orange / Ethidium bromide staining for apoptosis

AL-1 cells were electroporated (approx. 150k cells) with expression vectors (GFP with β-gal, axolotl Smad3 or axolotl Smad3 SΔD, see sup. table 3) and plated in a 12 well plate. Cells were harvested 48h post-electroporation and stained with Acridine Orange / Ethidium bromide as described in Ribble et al, 2005 and Kasibhatla et al, 2006 (Ribble et al., 2005; Kasibhatla et al., 2006).

TUNEL assay

Following injection and electroporation of plasmids (details for in situ electroporation can be found in Guimond et al 2010)(Guimond et al., 2010), 10 µm sections of paraffin embedded limbs were rehydrated then treated with Proteinase K 20µg/ml (Invitrogen, Ref#25530-015) for 20min at RT. Positive control were treated with DNAse 1 1U/50µL (Invitrogen,

ref#18068-015) for 10min at RT. Sections were then rinsed in TBS then TdT buffer 1X (Invitrogen, ref#16314-015) and treated with recombinant terminal deoxynucleotidyl transferase (TdT) 3,75U/µL (Invitrogen, ref#10533-065), Digoxigenin-11-dUTP 2µM (Roche, ref#11093088910) in TdT buffer 1X for 1h at 37°C. Slides were rinsed in TBS then blocking was performed at RT for 15min with 2% sheep serum in TBS. Slides were incubated with a primary Antibody against digoxigenin 1/1500 (Roche, ref#113333062910) at 4°C overnight. Slides were rinsed (4X 15min) with PBST then incubated with a secondary antibody coupled to Alexa fluor 594 (anti-mouse 1/250) (Invitrogen, ref#A11020) in blocking solution for 2h at RT in the dark. Slides were rinsed (4X15min) with PBST and mounted with ProLong® Gold antifade regent containing DAPI (Invitrogen, ref#36931). Slides were visualized with a Zeiss Axio Imager M2 Optical Microscope and composite images were generated (Zeiss, Munich, Germany).

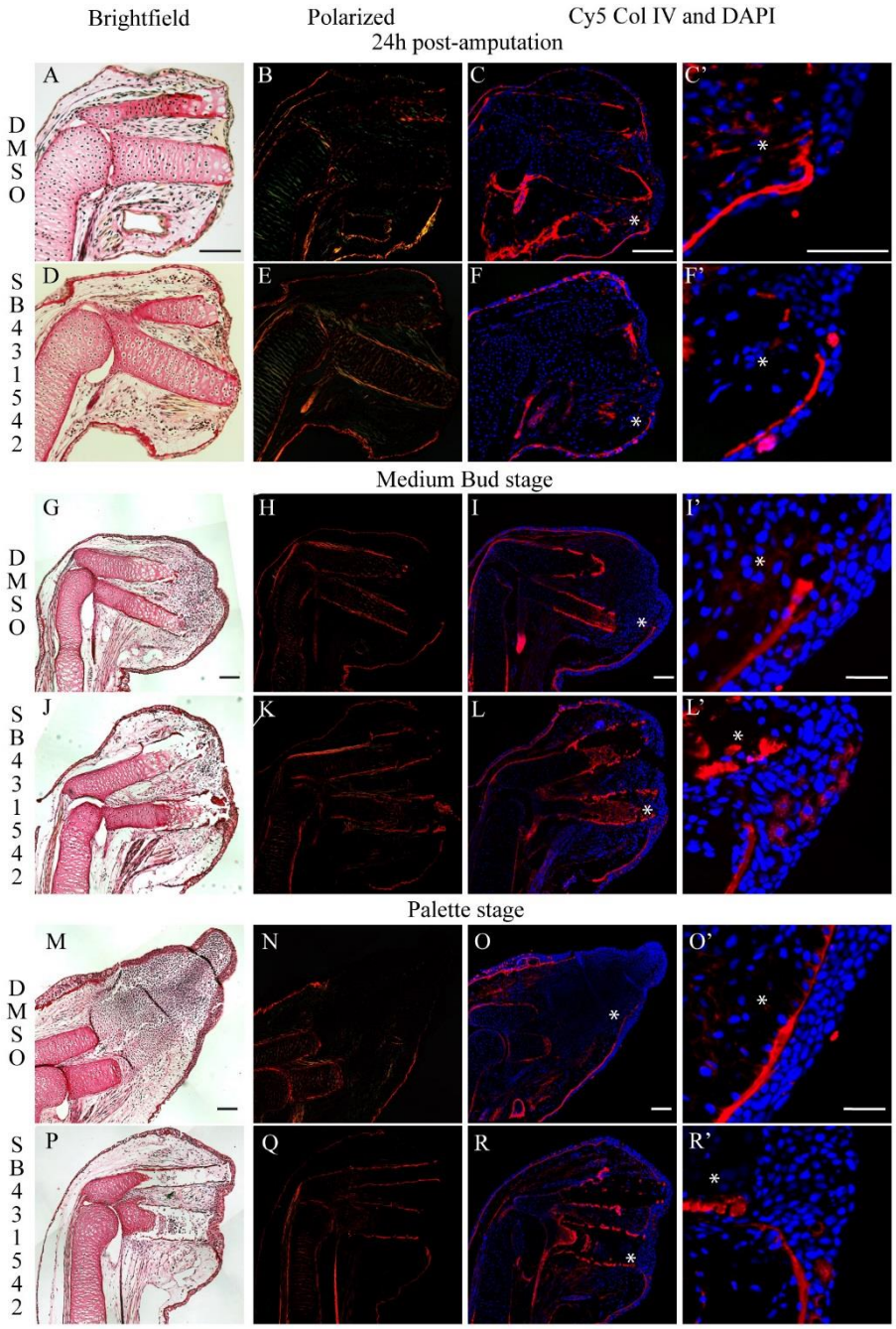

Supplementary Figure 1: **SB-431542 does not affect basement membrane reformation in regenerating limbs**

(**A-C**, **G-I**, **M-O**) Animals treated with DMSO (**A**,**G**,**M**) Brightfield view of limb indicates that a blastema is forming normally. Polarized light show some collagen deposition in Palette stage (**N**) in basement membrane region but not at 24h (**B**) or MB stage (**H**). Col IV expression (red) shows some collagen deposition in Palette stage (**O**,**O'**) in basement membrane region but not at 24h (**C**, **C'**) or MB stage (**I**,**I'**). (**D-F**, **J-L**, **P-R**) Animals treated with 25μM SB-431542 (**D**,**J**,**P**) Brightfield view of limb indicates that no blastema is forming. Polarized light show some collagen deposition in Palette stage (**Q**) in basement membrane region but not at 24h (**E**) or MB stage (**K**). Col IV expression (red) shows some collagen deposition in Palette stage (**R**,**R'**) in basement membrane region but not at 24h (**F**, **F'**) or MB stage (**L**,**L'**). Results show that basement membrane is not restored prematurely in limbs treated with SB-431542. Scale bar 200μM (**A**,**C**,**G**,**I**,**M**,**O**) and 60μM (**C'**,**I'**,**O'**). Composite images are shown and stars indicate areas of magnification.

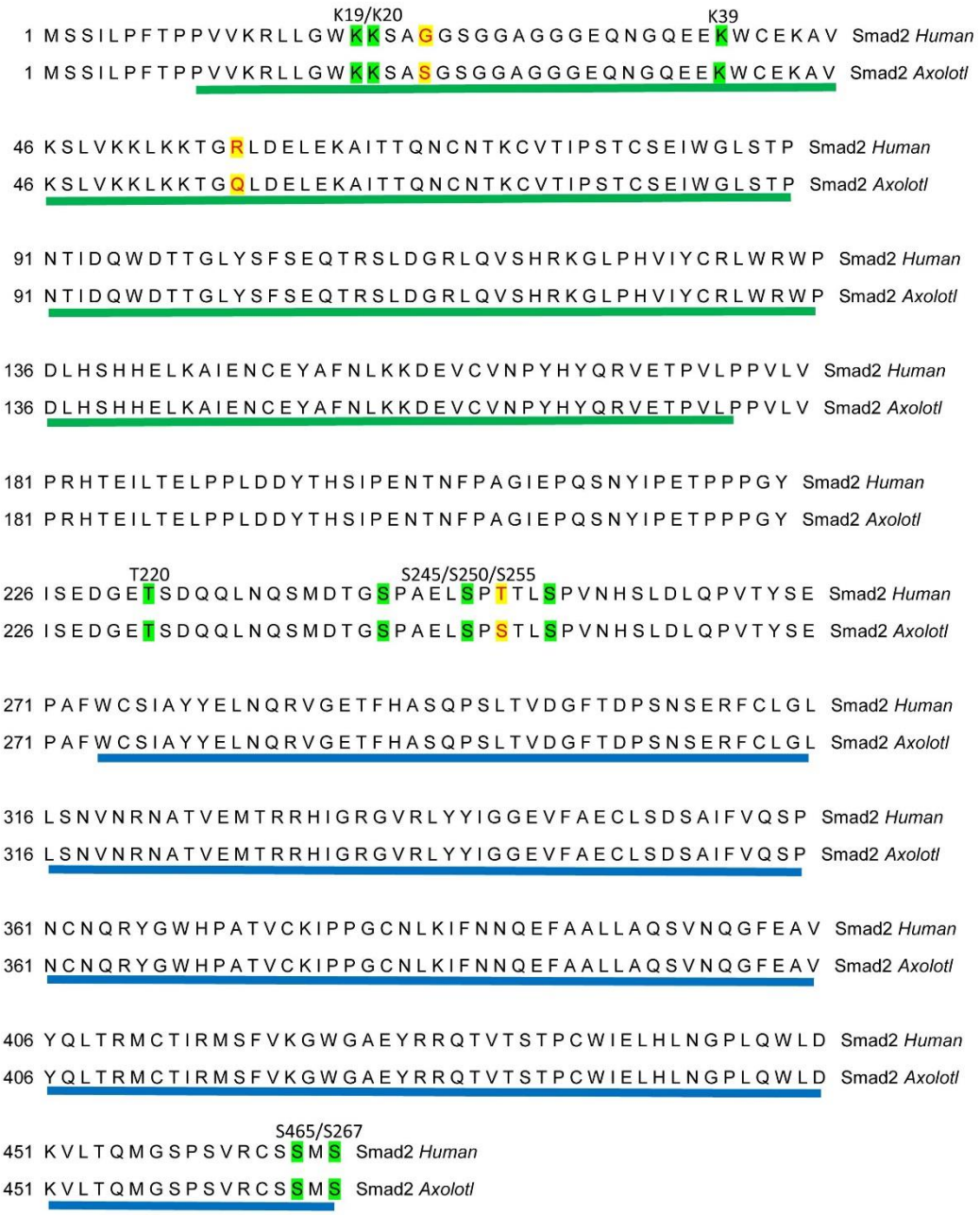

Supplementary Figure 2: **Protein alignment of Smad2**

Protein sequences for human and axolotl Smad2 were aligned using DNASTAR MegAlign. Sequences are greatly conserved between species. The axolotl Smad2 sequence has 99% identity with the human Smad2. MH1 domain is underlined in green. MH2 domain is underlined in blue. Linker domain is located between MHI and MH2 domain, with no underlining. Important post-translational modification sites are indicated on top of the aligned sequences and highlighted in green. Differences in aa are highlighted in yellow with red writing. All post-translational modification sites are conserved between both species.

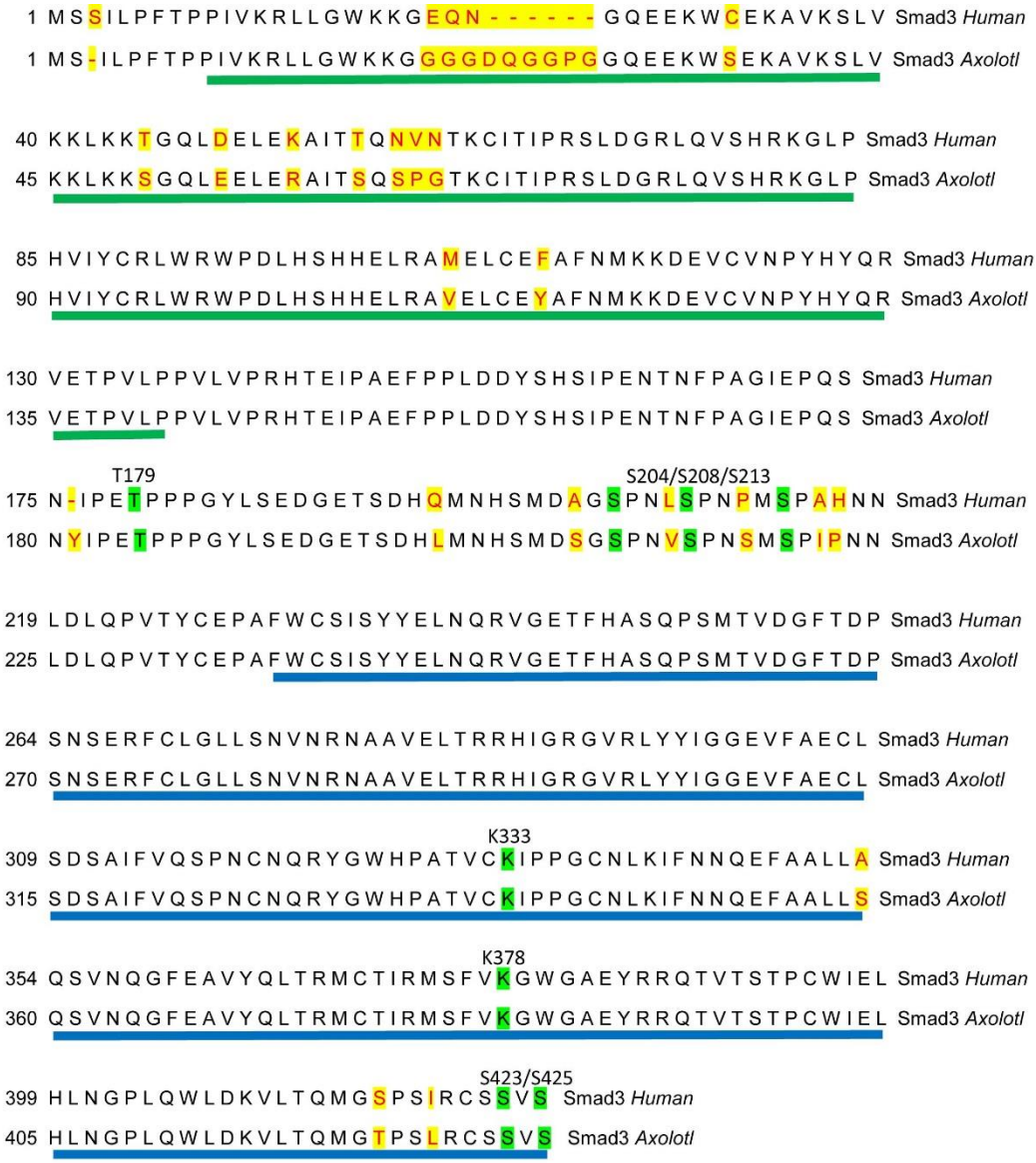

Supplementary Figure 3: **Protein alignment of Smad3**

Protein sequences for human and axolotl Smad3 were aligned using DNASTAR MegAlign. Sequences are greatly conserved between species. The axolotl Smad3 sequence has 93% identity with the human Smad3. MH1 domain is underlined in green. MH2 domain is underlined in blue. Linker domain is located between MHI and MH2 domain, with no underlining. Important post-translational modification sites are indicated on top of the aligned sequences and highlighted in green. Differences in aa are highlighted in yellow with red writing. All post-translational modification sites are conserved between both species.

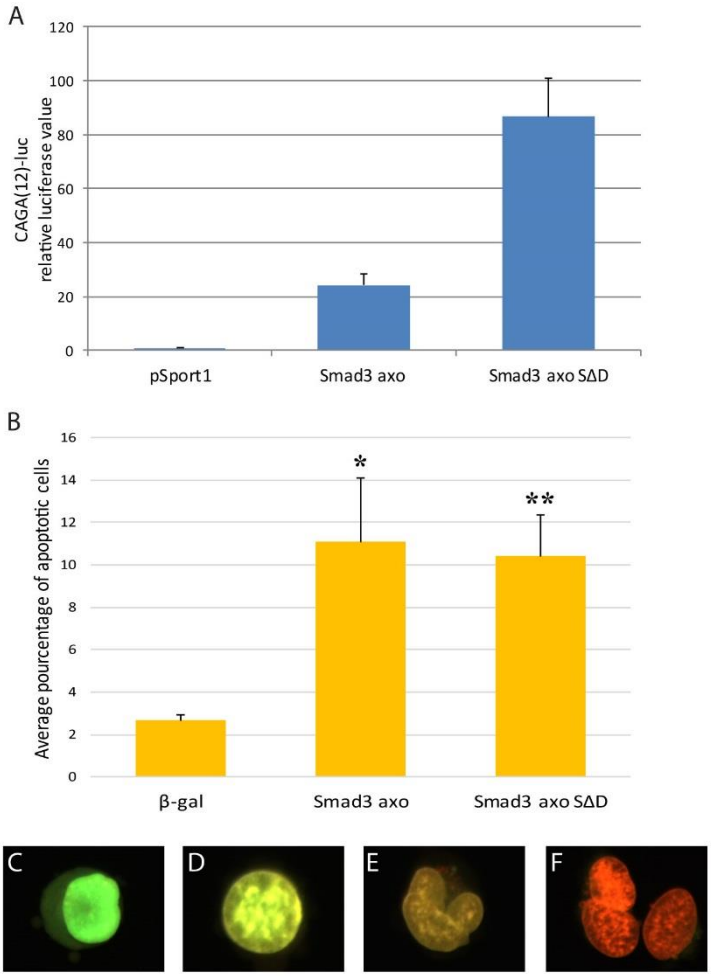

Supplementary Figure 4: **Overexpression of axolotl Smad3 leads to increased apoptosis in AL-1 cell line**

(**A**) Luciferase assay showing that axolotl Smad3 (Smad3 axo) and axolotl Smad3 SΔD (Smad3 axo SΔD, a phosphomimetic Smad3) overexpression have more activity on the CAGA promoter driving luciferase in AL-1cells than control vector (pSport1) (n=12). Data is presented as mean relative luciferase value ± SEM. (**B**) Acridine Orange/Ethidium Bromide double staining cell count for apoptosis; (**C**) viable cell (not counted), (**D**) early apoptosis (counted as apoptotic), (**E**) late apoptosis (counted as apoptotic) and (**F**) necrotic cells (not counted). Data is presented as mean percentage ± SEM. Student's t-test were performed to compare means. There is significantly more apoptosis in axolotl Smad3 and axolotl Smad3 SΔD compared to β-gal (**p< 0.01, * p < 0.05, n=3).

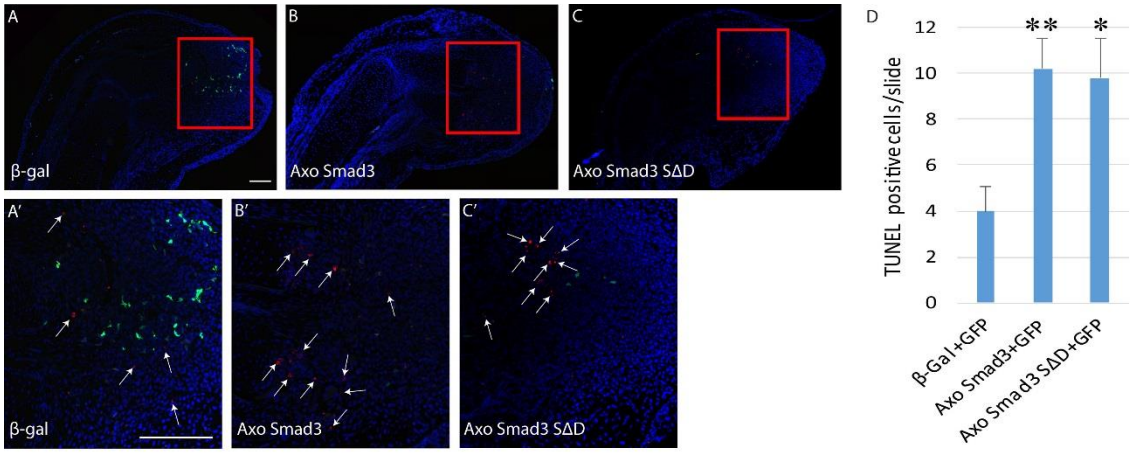

Supplementary Figure 5: **Overexpression of axolotl Smad3 in vivo leads to apoptosis**

(**A**-**A′**) Co-injection and electroporation of β-gal and GFP. Multiple fluorescent cells can be seen. Only a few cells are positive for apoptosis (TUNEL, 4 days post-transfection). (**B**-**B′**) Co-injection and electroporation of axolotl Smad3 and GFP. GFP positive cells are almost absent from slide. Multiple cells near the injection site are positive for apoptosis (TUNEL, 4 days post-transfection). (**C**-**C′**) Co-injection and electroporation of axolotl Smad3 SΔD and GFP. Similar results to what is observed for axolotl Smad3 presented in B and B′, GFP positive cells are almost absent from slide. Multiple cells near the injection site are positive for apoptosis (TUNEL, 4 days post-transfection). Regions in red square are magnified (**A′**, **B′**, **C′**). TUNEL positive cells (red) are pointed with arrows. Composite images are shown and scale bars represent 200μm. (**D**) TUNEL positive cells were counted for each condition (n=5 different animals). Data is presented as number of positive cells ± SEM. There are less apoptotic cells in β-gal and GFP co-injected blastemas compared to axolotl Smad3 and GFP or axolotl Smad3 SΔD and GFP co-injected blastemas. Welch's t-test was performed to compare apoptosis between different treatments; observed difference are statistically significant. ** $p < 0.01$, * $p < 0.05$.

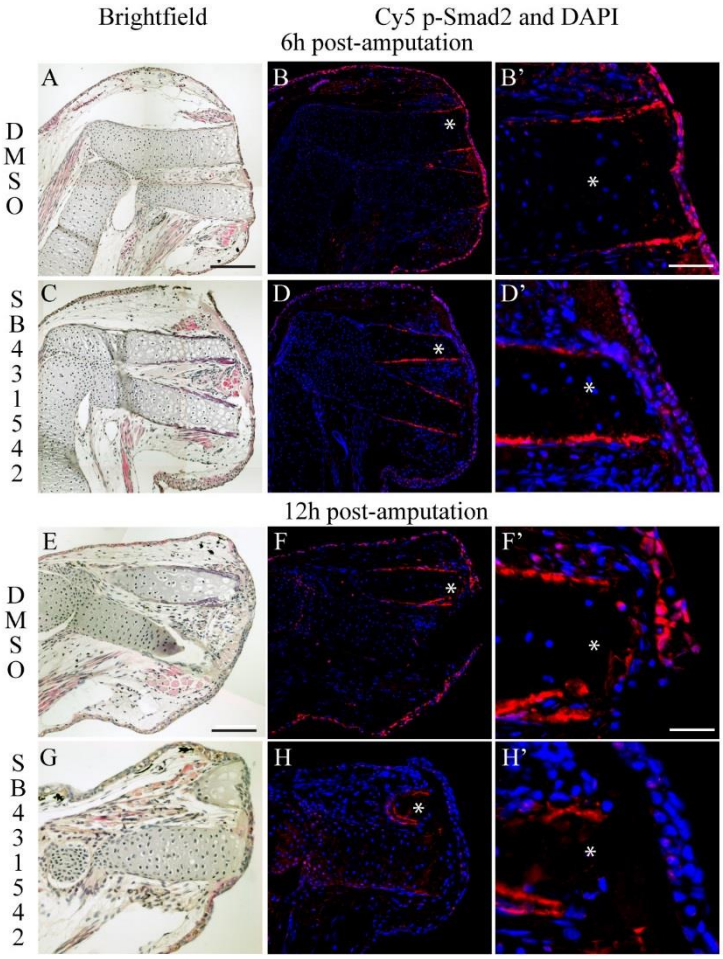

Supplementary Figure 6: **SB-431542 prevents phosphorylation of p-Smad2 in regenerating limbs**

Control animal treated with DMSO for 6h (**A**-**B**) or 12h (**E**-**F**). (**A**,**E**) Hematoxylin and Eosin staining shown in brightfield microscopy. Scale bar is 200µm. (**B**,**F**) Nuclei staining with DAPI (blue) overlaid with immunofluorescence of p-Smad2 (red) shows phosphorylation in most epithelial cells of the wound epithelium and some in the underlying mesenchymal cells. (**B'**,**F'**) Magnified view (Scale bar 50µm, composite images are shown and stars indicate area of magnification). Phosphorylated proteins are often in the nucleus. Animal treated with 25µM SB-431542 for 6h (**C**-**D**) or 12h (**G**-**H**) . (**C**,**G**) Hematoxylin and Eosin staining shown in brightfield microscopy. (**D**-**D'**, **H**-**H'**) Overlay of DAPI and immunofluorescence of p-Smad2 shows very limited positive cells for phosphorylated Smad2 protein. Composite images are shown and stars indicate area of magnification.

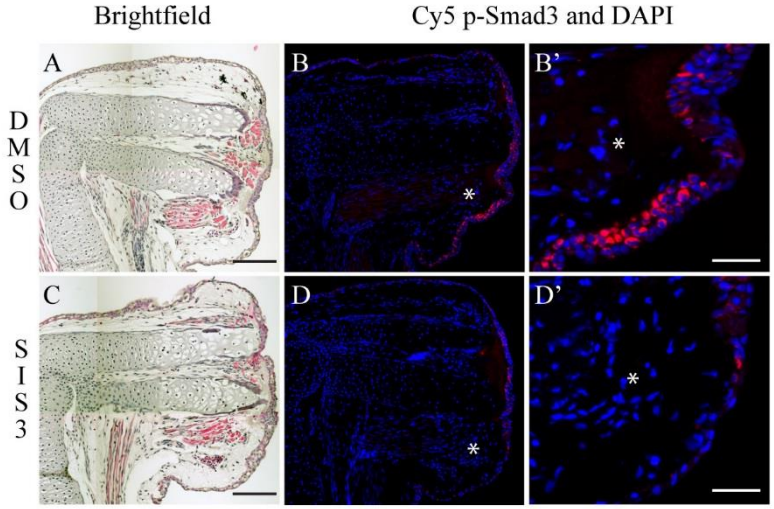

Supplementary Figure 7: **SIS3 treatment reduces phosphorylation of p-Smad3**

(**A**-**B**) Control animal treated for 3h with DMSO. (**A**) Hematoxylin and Eosin staining shown in brightfield microscopy. Scale bar is 300µm. (**B**) Overlay of nuclei staining with DAPI (blue) and immunofluorescence of p-Smad3 (red) shows phosphorylation in epithelial cells of the wound epithelium, especially near the plane of amputation. (**B'**) Magnified view (scale bar is 60µm, composite images are shown and stars indicate area of magnification) shows that phosphorylated proteins are often in the nucleus (pink). (**C**-**D**) Animal treated for 3h with 5µM SIS3. (**C**) Hematoxylin and Eosin staining shown in brightfield microscopy. Scale bar is 300µm. (**D**-**D'**) Overlay of nuclei staining with DAPI (blue) and immunofluorescence of p-Smad3 (red) shows reduced number of positive cells for phosphorylated Smad3 protein and (**D'**) p-Smad3 signal is not localized in nucleus. Scale bar is 60µm. Composite images are shown and stars indicate area of magnification.

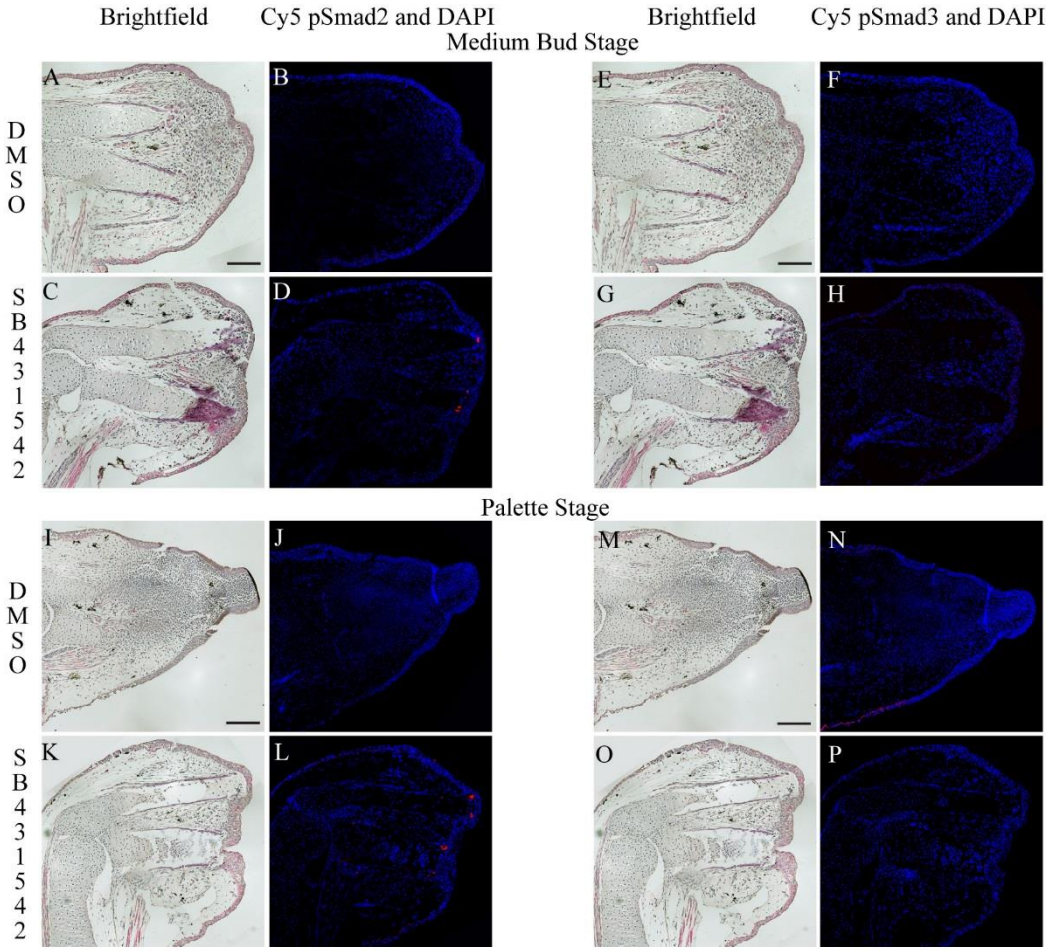

Supplementary Figure 8: **p-Smad2 and p-Smad3 are not detected at Medium Bud and Palette stages**

Control animal treated with DMSO until MB (**A**-**B**, **E**-**F**) or Pal (**I**-**J**,**M**-**N**). (**A**,**E**,**I**,**M**) Hematoxylin and Eosin staining shown in brightfield microscopy. Composite images are shown and scale bars are 200µm. (**B**,**F**,**J**,**N**) Nuclei staining with DAPI (blue) overlaid with immunofluorescence of p-Smad2 (**B**,**J**) or p-Smad3 (**F**,**N**) shows no phosphorylation. **Animal treated with 25µM SB-431542** until MB (**C**-**D**, **K**-**L**) or Pal (**G**-**H**, **O**-**P**). (**C**,**G**,**K**,**O**) Hematoxylin and Eosin staining shown in brightfield microscopy. (**D**,**H**,**L**,**P**) Overlay of DAPI and immunofluorescence shows no positive cells for phosphorylated proteins.

Supplementary Table 1: List of primers

Gene Name		Primer sequence 5' to 3'
Smad3 probe primers	3RSmd3-11 (forward)	AATCAGGGTTTCGAAGCCGT
	5RSmd3-5 (reverse)	CTGATTTACAGATTGGGACAA
Axolotl Smad2 (used for probe)	aSmd2F59	ATTCAGAACCAGCGTTTTGG
	aSmd2R598	ATTGCAGAGGTCCATTCAGG
Axolotl Smad3	Smad3_axo_F515	GGAGCTCTGCGAGTATGCCT
	Smad3_axo_R997	CTCTCCCACTCGTTGATTAAGC
Axolotl Smad7 (used for probe)	aSmd7F95	GCCTTCCTCCACTGAAACTG
	aSmd7R445	GTGGCCGACTTGATGAAAAT
Axolotl MMP2	aMMP2F100	TCAGAAGGCTCTCCCTGTGT
	aMMP2R779	GCTGCATCCACATGTTTCAC
Axolotl MMP9	F485_MMP9axo	AAGGGGGCTTGCAGGATAA
	R1091_MMP9axo	AGCACAGAAGTGTGGGCTCT
Axolotl MMP13	F2381_MMP13axo	AAAACGACGCTCCAAAACAC
	R2565_MMP13axo	AAGGCACACTCTCAGCCAAA
Axolotl MMP14	F2795_MMP14axo	TGGATAACTGAATGTGCGGA
	R3046_MMP14axo	GACGCTGACACTCAACCTCA
Axolotl GAPDH	aGAPDHF709	AGCTCAATGGGAAACTCACTGGC
	aGAPDHR966	TCACAAAGTGATCGTTGAGGGCA

Supplementary Table 2: Antibodies and blotting conditions

Antibody	Manufacturer	Ref #	Dilution	Conditions	Blocking	ECL
Smad2	Cell Signaling	5339	1/500	O.N. 4°C	5% milk in PBST, 6h 4°C	GE*
p-Smad2	Cell Signaling	3108	1/500	O.N. 4°C	5% chicken serum, 0,75% BSA in TBST, 1h30 RT	LL+**
Smad3	Zymed	51-1500	1/500	O.N. 4°C	5% milk in PBST, 6h 4°C	GE*
p-Smad3	*See materials and methods*	N/A	1/2500	O.N. 4°C	5% chicken serum, 0,75% BSA in TBST, 1h30 RT	SFE***
TGF-β1	Santa Cruz	Sc-146	1/500	O.N. 4°C	5% chicken serum, 0,75% BSA in TBST, 1h30 RT	GE*
GAPDH	Sigma	G8795	1/1000	1h RT	5% chicken serum in PBST, 1h RT	GE*

*Western blotting detection reagents, GE Healthcare, ref#RPN2109, Buckinghamshire, UK

**Lumi-Light^{Plus} Western Blotting Substrate, Roche, ref#12015196001

***SignalFire^{TM} Elite ECL Reagent, Cell Signaling, ref#12757

Supplementary Table 3: Plasmids used in injection/electroporation experiment

Gene expressed by plasmid with CMV promoter	Backbone	Quantity used (µg)
GFP	Max GFP	0.5
β-gal	pSport1	1
axolotl Smad3 (wild type)	pSport1	1
Axolotl Smad3 SΔD (Serine 423-425 mutated to glutamic acids)	pSport1	1

Supplementary References:

Guimond, J. C., Levesque, M., Michaud, P. L., Berdugo, J., Finnson, K., Philip, A. and Roy, S. (2010). BMP-2 functions independently of SHH signaling and triggers cell condensation and apoptosis in regenerating axolotl limbs. *BMC Dev Biol* **10**, 15.
Kasibhatla, S., Amarante-Mendes, G. P., Finucane, D., Brunner, T., Bossy-Wetzel, E. and Green, D. R. (2006). Acridine Orange/Ethidium Bromide (AO/EB) Staining to Detect Apoptosis. *CSH Protoc* **2006**.
Ribble, D., Goldstein, N. B., Norris, D. A. and Shellman, Y. G. (2005). A simple technique for quantifying apoptosis in 96-well plates. *BMC Biotechnol* **5**, 12.